Delaunay triangulations and cycles on closed hyperbolic surfaces

Mikhail Bogdanov, Monique Teillaud

Delaunay triangulations and cycles on closed hyperbolic surfaces

Mikhail Bogdanov, Monique Teillaud

RESEARCH REPORT
N° 8434
December 2013
Project-Team Geometrica

ISSN 0249-6399 ISRN INRIA/RR--8434--FR+ENG

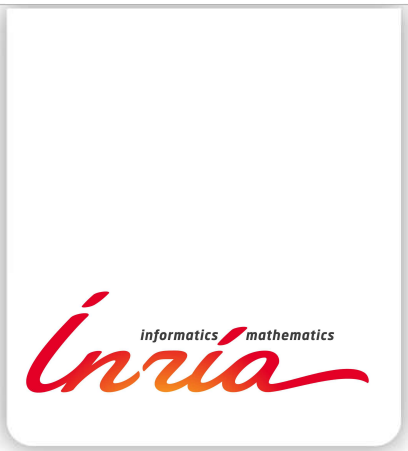

Delaunay triangulations and cycles on closed hyperbolic surfaces

Mikhail Bogdanov, Monique Teillaud

Project-Team Geometrica

Research Report n° 8434 — December 2013 — 26 pages

Abstract: This work is motivated by applications of *periodic* Delaunay triangulations in the Poincaré disk conformal model of the hyperbolic plane $\mathbb{H}^2$. A periodic triangulation is defined by an infinite point set that is the image of a finite point set by a (non commutative) discrete group Γ generated by hyperbolic translations, such that the hyperbolic area of a Dirichlet region is finite (i.e., a cocompact Fuchsian group acting on $\mathbb{H}^2$ without fixed points).
We consider the projection of such a Delaunay triangulation onto the closed orientable hyperbolic surface $M = \mathbb{H}^2/\Gamma$. The graph of its edges may have cycles of length one or two. We prove that there always exists a finite-sheeted covering space of M in which there is no cycle of length ≤ 2. We then focus on the group defining the Bolza surface (homeomorphic to a torus having two handles), and we explicitly construct a sequence of subgroups of finite index allowing us to exhibit a covering space of the Bolza surface in which, for any input point set, there is no cycle of length one, and another covering space in which there is no cycle of length two. We also exhibit a small point set such that the projection of the Delaunay triangulation on the Bolza surface for any superset has no cycle of length ≤ 2.
The work uses mathematical proofs, algorithmic constructions, and implementation.

Key-words: hyperbolic plane, hyperbolic translation, Delaunay triangulation, hyperbolic surface, Fuchsian group, covering space, algebraic software

RESEARCH CENTRE
SOPHIA ANTIPOLIS – MÉDITERRANÉE

2004 route des Lucioles - BP 93
06902 Sophia Antipolis Cedex

Triangulations de Delaunay et cycles sur des surfaces hyperboliques fermées

Résumé : Ce travail est motivé par les applications des triangulations de Delaunay *périodiques* dans le modèle du disque de Poincaré, modèle conforme du plan hyperbolique $\mathbb{H}^2$. Une triangulation périodique est définie par un ensemble infini de points, image d'un ensemble fini par un groupe discret (non commutatif) Γ engendré par des translations, et tel que l'aire hyperbolique d'un domaine de Dirichlet soit finie (c'est-à-dire un groups fuchsien cocompact agissant sur $\mathbb{H}^2$ sans point fixe).

Nous considérons la projection d'une telle triangulation de Delaunay sur la surface hyperbolique fermée orientable $M = \mathbb{H}^2/\Gamma$. Le graphe des arêtes de cette projection peut avoir des cycles de longueur un ou deux. Nous démontrons qu'il existe toujours un revêtement fini de M dans lequel il n'y a pas de cycle de longueur ≤ 2. Nous nous concentrons ensuite sur le groupe définissant la surface de Bolza (homéomorphe à un tore à deux anses), et nous construisons explicitement une suite de sous-groupes d'indice fini nous permettant d'exhiber un revêtement de la surface de Bolza dans lequel, quel que soit l'ensemble de points, il n'y a aucun cycle de longueur un, et un autre revêtement dans lequel il n'y a aucun cycle de longueur deux. Nous présentons aussi un petit ensemble de points tel que la projection de la triangulation de Delaunay de tout sur-ensemble sur la surface de Bolza n'a aucun cycle de longueur ≤ 2.

Ce travail utilise des démonstrations mathématiques, des constructions algorithmiques, et de la programmation.

Mots-clés : plan hyperbolique, translation hyperbolique, triangulation de Delaunay, surface hyperbolique, groupe fuchsien, revêtement, logiciel algébrique

1 Introduction

Periodic hyperbolic Delaunay triangulations, which can also be seen as triangulations on hyperbolic surfaces, are used in very diverse fields [29, 28, 4, 15].

The case of closed Euclidean manifolds was already addressed [12, 11, 13], leading to software packages for the flat torus in 2D and 3D [23, 14]. The algorithm follows the classic incremental algorithm in $\mathbb{E}^d$: for each new point p, the set of conflicting simplices (i.e., simplices whose balls contain p) is first computed, and the region that they form is then triangulated with new simplices with apex p. That algorithm relies on the fact that the set of conflicting simplices is always a topological ball. This subsumes that the Delaunay triangulation is a simplicial complex, which is the case when the graph of its edges has no cycle of length ≤ 2.

We study the case of a closed orientable hyperbolic surface M, isometric to a quotient $\mathbb{H}^2/\Gamma$, where Γ is a cocompact Fuchsian group acting on $\mathbb{H}^2$ without fixed points; π denotes the natural projection of $\mathbb{H}^2$ onto M that maps each point to its orbit under Γ. For a finite point set $\mathcal{P}$ in $\mathbb{H}^2$, we consider the Delaunay triangulation $\mathrm{DT}_{\mathbb{H}}(\Gamma\mathcal{P})$ of the infinite point set $\Gamma\mathcal{P}$ and its projection onto M. The graph of edges of $\pi(\mathrm{DT}_{\mathbb{H}}(\Gamma\mathcal{P}))$ can have non-trivial cycles of length one *(1-cycles)* or two *(2-cycles)*: for instance, in the extreme case when $\mathcal{P}$ consists of only one point p, then the set $\Gamma\mathcal{P}$ is the orbit of p under Γ, so, all vertices of its Delaunay triangulation in $\mathbb{H}^2$ project to the same point of M, i.e., each of its edges projects to a 1-cycle.

In Section 3, we give general conditions under which $\pi(\mathrm{DT}_{\mathbb{H}}(\Gamma\mathcal{P}))$ has no 1- or 2-cycles. We prove that there is always a finite-sheeted covering space $\widetilde{M_1}$ (resp. $\widetilde{M_2}$) of M in which, for any set $\mathcal{P}$, there is no 1-cycle (resp. no 2-cycle). Then we focus on the specific case of the Bolza surface $\mathcal{M}$, homeomorphic to the double torus. We give properties of fundamental domains and of closed geodesics in Section 4. In Section 5, we propose a way to construct some finite-sheeted covering spaces, and we exhibit a 4-sheeted covering space in which the projection of a Delaunay triangulation never has 1-cycles, and a 128-sheeted covering space in which it never has 2-cycles. While this has theoretical interest, we turn back to a more practical point of view in Section 6.

2 Background

For general algebraic and topologic notions, we refer the reader to textbooks such as [31, 1].

Isometries in the Poincaré disk model of the hyperbolic plane
In the *Poincaré disk model* ([10],[5, Chapter 19]) the hyperbolic plane $\mathbb{H}^2$ is represented as the open unit ball $\mathcal{B}$ of the Euclidean plane $\mathbb{E}^2$. The points on the boundary of $\mathcal{B}$ are the *points at infinity*, their set is denoted as $\mathcal{H}_\infty = \{x \in \mathbb{E}^2 : \|x\| = 1\}$. Hyperbolic lines, or geodesics, are represented either as arcs of Euclidean circles orthogonal to $\mathcal{H}_\infty$ or as diameters of $\mathcal{B}$. See Figure 1(Left).

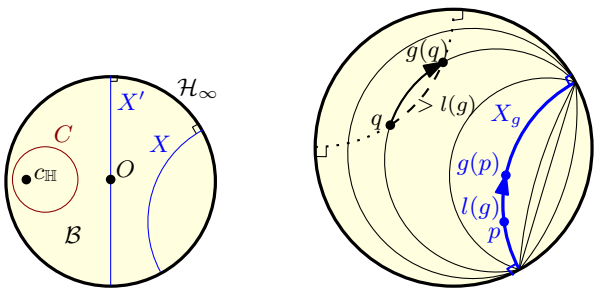

Figure 1: The Poincaré disk model. (Left) lines and circles. (Right) translation g of axis X_g.

As the Poincaré disk is a conformal model of the hyperbolic plane, it is widely used in applications [21, 29, 28, 4, 15].

The group of isometries of $\mathbb{H}^2$ is denoted as $\mathrm{Isom}(\mathbb{H}^2)$, and the group of orientation-preserving isome-

tries is denoted as $\text{Isom}^+(\mathbb{H}^2)$. Each $g \in \text{Isom}^+(\mathbb{H}^2)$ is of the form

$$g(z) = \frac{\alpha z + \beta}{\overline{\beta} z + \overline{\alpha}}, \text{ identified with matrix } \begin{bmatrix} \alpha & \beta \\ \overline{\beta} & \overline{\alpha} \end{bmatrix}, \text{ where } \alpha, \beta \in \mathbb{C}, |\alpha|^2 - |\beta|^2 = 1. \quad (1)$$

There are three types of orientation-preserving isometries of $\mathbb{H}^2$:

- *Elliptic.* An elliptic isometry, also called *rotation*, fixes one point of $\mathcal{B}$, the center of rotation.
- *Parabolic.* A parabolic isometry, also called *limit rotation*, fixes no point of $\mathcal{B}$ and fixes a unique point of the circle at infinity $\mathcal{H}_\infty$. It permutes the lines ending at the fixed point and preserves the Euclidean circles tangential to the boundary of $\mathcal{B}$ at the fixed point.
- *hyperbolic.* A hyperbolic isometry, also called *translation*, fixes no point of $\mathcal{B}$ and fixes two points on $\mathcal{H}_\infty$. The *axis* X_g of a translation g is the hyperbolic line ending at the two fixed points. The translation g translates any point along a curve at constant distance to the axis. All such curves have the fixed points of g as infinite points. The distance by which the translation g moves all points of the axis is the same, it is called the *translation length* $l(g) = 2 \cdot acosh\left(\frac{1}{2}Tr(g)\right)$ of g, where $Tr(g)$ is the trace of the matrix representing g. If a point p is not on the axis of g, then the distance by which g moves p is strictly greater than $l(g)$. See Figure 1(Right).

  Note that two translations do not commute in general.

Fuchsian groups, hyperbolic surfaces, Dirichlet regions

For more details, we refer to the literature [22, 33, 34, 36, 35].

A *Fuchsian group* is a discrete subgroup of $\text{Isom}^+(\mathbb{H}^2)$. A *hyperbolic surface* is a connected 2-dimensional manifold, such that every point has a neighborhood isometric to a disk of $\mathbb{H}^2$. A compact hyperbolic surface is called *closed*. As a consequence of the Killing-Hopf theorem [27, Theorem 8.5.9], any closed orientable hyperbolic surface M is isometric to a quotient $\mathbb{H}^2/\Gamma$, where Γ is a Fuchsian group acting on $\mathbb{H}^2$ without fixed points. Since Γ acts on $\mathbb{H}^2$ without fixed points, it contains no elliptic element; the compactness of M implies that Γ contains no parabolic element [27, Theorem 6.6.6]. To summarize,

> *a closed orientable hyperbolic surface M is of the form $\mathbb{H}^2/\Gamma$,*
> *where Γ is a Fuchsian group only containing hyperbolic translations.*

The projection map $\pi : \mathbb{H}^2 \to M = \mathbb{H}^2/\Gamma$ is a local isometry and a covering projection. The *Dirichlet region* $\mathcal{D}_p(\Gamma)$ for Γ centered at p is defined as the closure of the open cell $V_p(\Gamma p)$ of p in the Voronoi diagram $\text{VD}_{\mathbb{H}}(\Gamma p)$ of Γp in $\mathbb{H}^2$. It is a compact convex polygon with finitely many sides (Siegel's theorem). The area of M is finite: $area(M) = 4\pi(genus(M) - 1)$. Each Dirichlet region $\mathcal{D}_p(\Gamma) = Cl(V_p(\Gamma p))$ is a *fundamental domain* for the action of Γ on $\mathbb{H}^2$, i.e., *(i)* $\bigcup_{g\in\Gamma} g(\mathcal{D}_p(\Gamma)) = \mathbb{H}^2$, and *(ii)* $\forall g_1, g_2 \in \Gamma, g_1 \neq g_2, g_1(Int(\mathcal{D}_p(\Gamma))) \cap g_2(Int(\mathcal{D}_p(\Gamma))) = \emptyset$.

Closed geodesics, systole, length spectrum

The *systole* $sys(M)$ is the least length of a non-contractible loop on M [20]. There are upper bounds depending on the area and the genus of M [19, 9]. Clearly, the shortest closed curves on M are simple curves. For a given closed non-contractible loop γ on M, there is a unique closed geodesic that is the shortest closed curve that can be continuously deformed into γ [33, 27]; as a consequence, the shortest closed curves on M are closed geodesics. The closed geodesics of a hyperbolic surface $M = \mathbb{H}^2/\Gamma$ are in one-to-one correspondence with the conjugacy classes of hyperbolic elements of Γ; The length of the closed geodesic γ corresponding to a conjugacy class $[h], h \in \Gamma$, is the translation length $l(h)$ [27]. The axis X_h projects to γ by π; it can be thought of as "winding" X_h on γ infinitely many times. Clearly, any gX_h, where $g \in \Gamma$, projects onto the same closed geodesic γ by π. The hyperbolic line gX_h is the axis of the translation ghg^{-1}.

Note that the conjugacy classes $[h]$ and $[h^2]$ are different; the closed geodesic corresponding to $[h^2]$ traverses twice the closed geodesic corresponding to $[h]$. An element $h \in \Gamma$ is called *primitive* in Γ if there is no element $g \in \Gamma$, such that $h = g^m, m \in \mathbb{Z} \setminus \{0\}$. The closed geodesics corresponding to primitive elements are also called *primitive*.

The *length spectrum* $L(\Gamma)$ of Γ is the ordered sequence of translation lengths of elements of Γ, i.e., the ordered sequence of lengths of the closed geodesics of M. The *multiplicity* of $l \in L(\Gamma)$ is the number of distinct conjugacy classes in Γ whose elements have the same length l, i.e., the number of different closed geodesics of the same length (the conjugacy classes $[h]$ and $[h^{-1}]$ are different, the corresponding closed geodesics are counted as different geodesics). The systole of M is the first element in $L(\Gamma)$.

3 Projecting $\mathrm{DT}_{\mathbb{H}}(\Gamma\mathcal{P})$ on a closed hyperbolic surface

Let $M = \mathbb{H}^2/\Gamma$ be a closed hyperbolic surface, with projection $\pi : \mathbb{H}^2 \to M$, and $\mathcal{P}$ a finite set of points in $\mathbb{H}^2$. Without loss of generality we assume that no two points of $\mathcal{P}$ lie on the same Γ-orbit, otherwise we can always choose a proper subset $\mathcal{P}' \subset \mathcal{P}$, so that $\Gamma\mathcal{P}' = \Gamma\mathcal{P}$. By definition, for any given point p, all elements of the orbit $\Gamma p = \{gp, g \in \Gamma\}$ project by π to the same point $\pi(p)$ of M.

Each $g \in \Gamma$ is an isometry, so, an empty disk circumscribing a triangle $(p, q, r), p, q, r \in \mathbb{H}^2$, is transformed by g into the disk circumscribing $(g(p), g(q), g(r))$, which is also empty. If the set $\Gamma\mathcal{P}$ shows degeneracies, i.e., subsets of four or more cocircular points, then the Delaunay triangulation of such a subset (a polygon) formed by cocircular points $P = (p_0, p_1, \ldots, p_k = p_0)$ is not uniquely defined. For any $g \in \Gamma$, the polygon $g(P) = (g(p_0), g(p_1), \ldots, g(p_k) = g(p_0))$ is also formed by cocircular points. Once a triangulation of P is chosen, the polygon $g(P)$ can be triangulated by the image of the polygon by g. Then these two triangulations project to the same set of triangles on M by π. From now on, we will consider that $\mathrm{DT}_{\mathbb{H}}(\Gamma\mathcal{P})$ is a partition of $\mathbb{H}^2$ by vertices, edges, and triangular (2-)faces.

Proposition 1. *Let σ be a face of $DT_{\mathbb{H}}(\Gamma\mathcal{P})$ and let $\breve{\sigma}$ be the face σ with punctured vertices. The restriction of π to $\breve{\sigma}$ is injective.*

Proof. $\mathrm{DT}_{\mathbb{H}}(\Gamma\mathcal{P})$ is a simplicial complex. Assume that the restriction of π to $\breve{\sigma}$ is not injective. Then there exist $p, q \in \breve{\sigma}$, $p \neq q$, such that $\pi(p) = \pi(q)$, or in other words $q = g(p)$ for some non-identity $g \in \Gamma$. Since $p \in \sigma$, then $g(p) \in g(\sigma)$. On the other hand $g(p) = q \in \sigma$. Thus $q \in \sigma \cap g(\sigma) = e_q$. Since $\mathrm{DT}_{\mathbb{H}}(\Gamma\mathcal{P})$ is a simplicial complex, e_q is an edge. The point q lies in the interior of that edge. Similarly, p lies in the interior of the edge $e_p = \sigma \cap g^{-1}(\sigma)$. See Figure 2. Since $q = g(p) \in g(e_p)$ in $\mathrm{DT}_{\mathbb{H}}(\Gamma\mathcal{P})$, $q \in e_q \cap g(e_p)$.

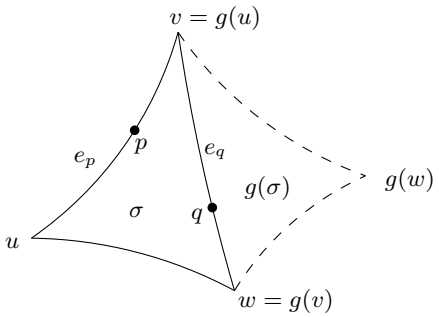

Figure 2: Proof of Proposition 1.

The edges e_q and $g(e_p)$ must coincide, since they intersect in the interior point. Since $e_q = g(e_p)$ and g is a translation, $e_q \neq e_p$. Let u, v, w be the vertices of σ as shown on the figure. Since $g(e_p) = e_q$, then either $g(v) = v$ or $g(v) = w$. Since g acts without fixed points on $\mathbb{H}^2$, $g(v) = w$. So, the image $g(u)$ is v. The faces σ and $g(\sigma)$ are adjacent through the edge e_q, so, the image $g(w)$ must be the vertex of $g(\sigma)$ opposite to e_q. The vertices u, v, w are oriented clockwise. Their images $g(u), g(v), g(w)$ are the vertices $v, w, g(w)$ respectively, which are oriented counterclockwise. This is a contradiction with the fact that g preserves orientation. □

If the restriction of π to σ is not injective, the image $\pi(\sigma)$ is an embedded geodesic triangle for which at least two vertices coincide, i.e., at least one of the edges of $\pi(\sigma)$ is in fact a 1-cycle.

Since π is surjective, the projection $\pi(\mathrm{DT}_{\mathbb{H}}(\Gamma\mathcal{P}))$ forms a partition of M by vertices, edges, and triangular faces.

Proposition 2. *(1) Any 1-cycle in the graph of edges of $\pi(DT_{\mathbb{H}}(\Gamma\mathcal{P}))$ is freely homotopic to a simple closed geodesic.*
(2) If a 2-cycle in the graph of edges of $\pi(DT_{\mathbb{H}}(\Gamma\mathcal{P}))$ is a union of two 1-cycles, then it is either freely homotopic to a closed geodesic with at most one transversal self-intersection or freely homotopic to a non-primitive closed geodesic traversing twice a simple closed geodesic. Otherwise, a 2-cycle is freely homotopic to a simple closed geodesic.

A 1-cycle e with a vertex v is a geodesic loop. Note that e is not necessary a closed geodesic: it may form an angle that is not π at vertex v.

Proof. Both results use the following [8]: the number of self-intersections of a closed non-contractible curve on M is at least the number of self-intersections of the closed geodesic in its free homotopy class. Then (1) follows from the previous paragraph: a 1-cycle is a geodesic loop without self-intersection. Now let ς be a 2-cycle formed by two edges ς_1 and ς_2 of $\pi(DT_{\mathbb{H}}(\Gamma\mathcal{P}))$. Consider the case when ς_1 and ς_2 are both 1-cycles. If they coincide, then clearly ς_2 is freely homotopic to a non-primitive closed geodesic traversing twice a simple closed geodesic. If the edges ς_1 and ς_2 do not coincide, then they are internally disjoint. The 2-cycle ς can be parametrized as a path with a transversal self-intersection; this path is freely homotopic to a closed geodesic with at most one transversal self-intersection. Consider the case when ς_1 is not a 1-cycle, then ς_2 is not a 1-cycle either. The edges ς_1 and ς_2 are internally disjoint, so, the 2-cycle ς does not have a self-intersection. When two geodesic paths with the same endpoints in M are homotopic, then they coincide, thus the distinct edges ς_1, ς_2 are not homotopic. So, the 2-cycle $\varsigma_1 \cup \varsigma_2$ is non-contractible. It does not have self-intersections, so must be freely homotopic to a simple closed geodesic. □

Largest empty disks and criteria.
Let us first consider disks that do not contain any element of the Γ-orbit of a given point p. The Voronoi diagram of Γp is the partition of $\mathbb{H}^2$ by the translated images of Dirichlet regions $\mathcal{D}_p(\Gamma)$ by the elements of Γ. Largest empty disks are centered at images of the vertices of $\mathcal{D}_p(\Gamma)$ that are furthest to p; δ_p denotes their diameter.

Let us define δ_M as $\delta_M = \sup\{\delta_z \mid z \in \mathcal{D}_O\}$, where O denotes the origin. δ_M is completely determined by the group Γ. The following inequality holds:

Proposition 3. $\delta_M \leq 2\delta_O$.

Proof. Let z be a point in $\mathbb{H}^2$. Let x be one of the vertices of $\mathcal{D}_z(\Gamma)$ furthest to z. We denote the disk centered at x with diameter δ_z by $B_x(\delta_z)$. By construction this disk is one of the largest disks whose interiors contain no point of Γz. The point x is contained in a Dirichlet region $\mathcal{D}_{O'}(\Gamma)$, for some $O' \in \Gamma O$. The distance from O' to any point of $\mathcal{D}_{O'}(\Gamma)$ is not greater than $\frac{1}{2}\delta_{O'}$, so, $dist_{\mathbb{H}}(x, O') \leq \frac{1}{2}\delta_{O'}$.

The Dirichlet region $\mathcal{D}_{O'}(\Gamma)$ must contain a point of the orbit Γz, say z'. The distance from O' to z' is not greater than $\frac{1}{2}\delta_{O'}$. Thus the disk $B_{O'}(\delta_{O'})$ centered at O' and of diameter $\delta_{O'}$ contains z'.

Since $dist_{\mathbb{H}}(x, O') \leq \frac{1}{2}\delta_{O'}$, the disk $B_{O'}(\delta_{O'})$ contains x. Since the disk $B_{O'}(\delta_{O'})$ contains both x and z', then $dist_{\mathbb{H}}(x, z') \leq \delta_{O'}$. By construction the disk $B_x(\delta_z)$ contains no point of Γz in its interior, so it does not contain z'. Thus the radius $\frac{1}{2}\delta_z$ of $B_x(\delta_z)$ is not greater than $dist_{\mathbb{H}}(x, z')$. So we have $\frac{1}{2}\delta_z \leq dist_{\mathbb{H}}(x, z') \leq \delta_{O'}$. Since $\delta_z \leq 2\delta_{O'}$ holds for any z, $\delta_M \leq 2\delta_{O'}$. It only remains to note that

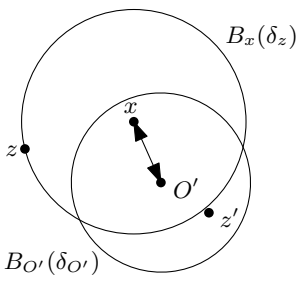

Figure 3: Proof of Proposition 11

$\delta_{O'} = \delta_O$. □

For a set of points $\mathcal{P}$, we denote as $\delta_{\mathcal{P}}$ the largest diameter of disks that do not contain any point of $\mathcal{P}$. Clearly, for $p \in \mathcal{P}$:

$$\delta_{\mathcal{P}} \leq \delta_p \leq \delta_M.$$

Proposition 4. *(1) If $sys(M) > \delta_{\mathcal{P}}$, then the graph of edges of $\pi(DT_{\mathbb{H}}(\Gamma\mathcal{P}))$ has no 1-cycle.*
(2) If $sys(M) > 2\delta_{\mathcal{P}}$, then the graph of edges of $\pi(DT_{\mathbb{H}}(\Gamma\mathcal{P}))$ has no 2-cycle.

Proof. (1) Assume that $sys(M) > \delta_{\mathcal{P}}$. For each edge e in $\mathrm{DT}_{\mathbb{H}}(\Gamma\mathcal{P})$ there exists an empty ball having the endpoints of e on its boundary. The length of the edge e is at most the diameter of the ball, so, it is not larger than $\delta_{\mathcal{P}}$. If the endpoints of $\pi(e)$ coincide, then $\pi(e)$ is a non-contractible geodesic loop, so, its length is not smaller than $sys(M)$ by definition, and we get a contradiction. (2) Assume now that $sys(M) > 2\delta_{\mathcal{P}}$ and there is a 2-cycle $\varsigma_1 \cup \varsigma_2$ in $\pi(\mathrm{DT}_{\mathbb{H}}(\Gamma\mathcal{P}))$. The length of the non-contractible loop $\varsigma_1 \cup \varsigma_2$ is the sum of the lengths of ς_1 and ς_2, and therefore is at most $2\delta_{\mathcal{P}}$, so we get a contradiction. □

Section 5 shows a covering of the Bolza surface in which the graph $\pi(DT_{\mathbb{H}}(\Gamma\mathcal{P}))$ has a 2-cycle formed by edges of length $\delta_{\mathcal{P}}$, i.e. $sys(M) = 2\delta_{\mathcal{P}}$. So, the criterion is sharp.

Covering spaces.
Let $\widetilde{\Gamma}$ be a subgroup of finite index k in Γ. The quotient space $\widetilde{M} = \mathbb{H}^2/\widetilde{\Gamma}$ is a closed hyperbolic surface. We denote as $\widetilde{\pi} : H^2 \to \widetilde{M}$ the projection map. Consider the map $f : \widetilde{M} \to M$ such that $\pi = f \circ \widetilde{\pi}$. The surface $\widetilde{M}$ is a k-sheeted covering space of M with f as a covering map and a local isometry. Note that then $Area(\widetilde{M}) = k \cdot Area(M)$, and $genus(\widetilde{M}) = k(genus(M) - 1) + 1$.

Proposition 5. *If $sys(\widetilde{M}) > \delta_M$, then for any $\mathcal{P}$, $\widetilde{\pi}(DT_{\mathbb{H}}(\Gamma\mathcal{P}))$ has no 1-cycle.*
If $sys(\widetilde{M}) > 2\delta_M$, then for any $\mathcal{P}$, $\widetilde{\pi}(DT_{\mathbb{H}}(\Gamma\mathcal{P}))$ has no 2-cycle.

Proof. Let $\widetilde{\mathcal{D}}_O$ be the Dirichlet region for $\widetilde{\Gamma}$ centered at O. Since Γ is discrete, the set $\widetilde{\mathcal{P}} = \widetilde{\mathcal{D}}_O \cap \Gamma\mathcal{P}$ is finite. Note that $\Gamma\mathcal{P} = \widetilde{\Gamma}\widetilde{\mathcal{P}}$, and as an obvious consequence $\widetilde{\pi}(DT_{\mathbb{H}}(\Gamma\mathcal{P})) = \widetilde{\pi}(DT_{\mathbb{H}}(\widetilde{\Gamma}\widetilde{\mathcal{P}}))$. The largest empty ball diameter $\delta_{\widetilde{\mathcal{P}}}$ for the point set $\widetilde{\Gamma}\widetilde{\mathcal{P}}$ is equal to $\delta_{\mathcal{P}}$, and thus it is at most δ_M. The rest is a simple consequence of Proposition 4. □

The main result of this section follows.

Proposition 6. *There exists a finite-sheeted covering space $\widetilde{M}_1$ of M such that $sys(\widetilde{M}_1) > \delta_M$.*
There exists a finite-sheeted covering space $\widetilde{M}_2$ of M such that $sys(\widetilde{M}_2) > 2\delta_M$.

Proof. We use the fact that for any $l_0 > 0$, only finitely many closed geodesics on M have length $\leq l_0$ [8]. These closed geodesics correspond to some conjugacy classes $[g_1], [g_2], \ldots, [g_{m(l_0)}]$ of Γ.

The group Γ is *residually finite*, as all Fuchsian groups are [24, 30], i.e., for each finite subset of Γ, there is a normal subgroup of finite index not containing the elements of that subset. So, there exists a normal subgroup $\widetilde{\Gamma}$ of finite index containing none of $g_1, g_2, \ldots, g_{m(l_0)}$. Since $\widetilde{\Gamma}$ is a normal subgroup, it contains no elements of $[g_1], [g_2], \ldots, [g_{m(l_0)}]$. As a consequence, there is no closed geodesic of length $\leq l_0$ on the surface $\mathbb{H}^2/\widetilde{\Gamma}$. □

The proof is constructive: there are algorithms to compute subgroups of index up to some fixed k in Γ that do not contain a given subset of elements of Γ. Using Proposition 5, these algorithms should compute subgroups giving covering spaces in which for any $\mathcal{P}$ the projection of $DT_{\mathbb{H}}(\Gamma\mathcal{P})$ has no 1- or no 2-cycle. The function `LowIndexSubgroupsFpGroup( G, H, index, excluded )`[1] of GAP [18] implements such an algorithm, due to Sims [32]. However, its important memory consumption does not allow us to use it for the Bolza surface in practice, so, we will propose our own construction in Section 5.

4 Bolza surface

Consider a regular octagon in $\mathbb{H}^2$ centered at the origin O and with angle $\pi/4$ at each vertex, and the four hyperbolic translations a, b, c, d that paiwise identify opposite sides of the octagon, as in Figure 4. They generate a Fuchsian group $\mathcal{G}$ for which the octagon is a fundamental domain. The Voronoi diagram $\mathrm{VD}_{\mathbb{H}}(\mathcal{G}O)$ can be seen on Figure 9(right).

[1] Γ is a finitely presented group

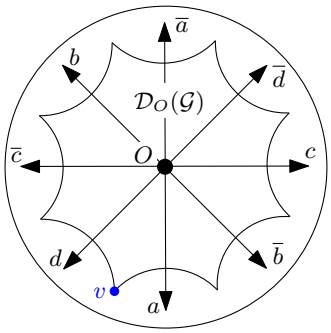

Figure 4: Translations a, b, c, d and their inverses.

The inverse of an element $g \in \mathcal{G}$ is denoted as $\overline{g}$. The group $\mathcal{G}$ can be written in the form of a *finitely presented group*

$$\mathcal{G} = \left\langle a, b, c, d \mid abcd\overline{a}\overline{b}\overline{c}\overline{d} \right\rangle,$$

i.e., the quotient of the group $\langle a, b, c, d\rangle$ generated by a, b, c, d, by the normal closure (i.e., the smallest normal subgroup) in $\langle a, b, c, d\rangle$ of the element $abcd\overline{a}\overline{b}\overline{c}\overline{d}$. The *Bolza surface* is $\mathcal{M} = \mathbb{H}^2/\mathcal{G}$. It is a closed orientable hyperbolic surface homeomorphic to a torus having two handles, i.e., a double torus.

4.1 Dirichlet regions

The first property of Dirichlet regions requires to quickly introduce triangle groups [33, 27].

For integers $p, q, r \geq 2$, $\frac{1}{p} + \frac{1}{q} + \frac{1}{r} < 1$, the *triangle group* $T(p, q, r)$ is defined as the group generated by reflections in the edges of the triangle $\Delta(p, q, r)$ whose angles are $\frac{\pi}{p}, \frac{\pi}{q}, \frac{\pi}{r}$. The triangles $\{g(\Delta(p, q, r)), g \in T(p, q, r)\}$ partition the plane $\mathbb{H}^2$.

The group $\mathcal{G}$ is a normal subgroup of index 16 without fixed points of $T(2, 8, 8)$. The triangle MNO with angles $\pi/2, \pi/8, \pi/8$ is a fundamental domain for $T(2, 8, 8)$ (Figure 5(left)). Repeated applications of reflections in its two edges incident to O form the fundamental domain of $\mathcal{G}$.

The group $\mathcal{G}$ is a normal subgroup of index 96 without fixed points of the triangle group $T(2, 3, 8)$. The group $T(2, 3, 8)$ is actually the largest subgroup of $Isom(\mathbb{H}^2)$ in which $\mathcal{G}$ is normal, i.e., $T(2, 3, 8) = \{t \in Isom(\mathbb{H}^2) \mid t\mathcal{G}t^{-1} = \mathcal{G}\}$. The projection map from $\mathbb{H}^2$ to $\mathcal{M}$ induces the partition of the surface $\mathcal{M}$ into triangles $\Delta(2, 3, 8)$. See Figure 5(right), where the small circles show elements of the orbit $T(2, 3, 8)O$.

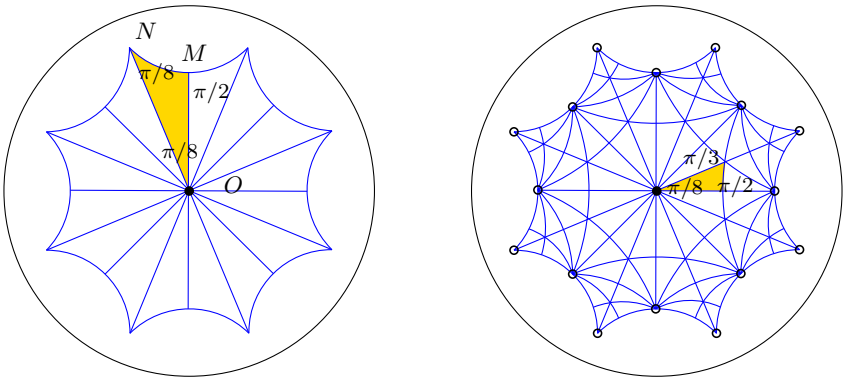

Figure 5: Partition of a fundamental domain for $\mathcal{G}$ into fundamental domains for the triangle groups $T(2, 8, 8)$ (left) and $T(2, 3, 8)$ (right).

Proposition 7. *If two points p and q of $\mathbb{H}^2$ lie in the same orbit under $T(2, 3, 8)$, then the Dirichlet regions $\mathcal{D}_p(\mathcal{G})$ and $\mathcal{D}_q(\mathcal{G})$ are isometric.*

Proof. Let $q = r(p)$ be the image of p under some isometry $r \in T(2,3,8)$. Since $\mathcal{G}$ is normal in $T(2,3,8)$, $r\mathcal{G}r^{-1} = \mathcal{G}$. Then $\mathcal{G}q = r\mathcal{G}r^{-1}q = r\mathcal{G}p$, i.e., the orbit $\mathcal{G}q$ is the image of the orbit $\mathcal{G}p$ under r. The Voronoi diagram $\mathrm{VD}_{\mathbb{H}}(\mathcal{G}q)$ is the image of $\mathrm{VD}_{\mathbb{H}}(\mathcal{G}p)$ under r. Therefore $\mathcal{D}_q(\mathcal{G}) = Cl(V_q(\mathcal{G}q))$ in $\mathrm{VD}_{\mathbb{H}}(\mathcal{G}q)$ is isometric to $\mathcal{D}_p(\mathcal{G})$. □

For simplicity, in the sequel we denote as g the image $g(O)$ of the origin by an element of $g \in \mathcal{G}$. We also label each side of $\mathcal{D}_p(\mathcal{G})$ by the translation of $\mathcal{G}$ that maps $\mathcal{D}_p(\mathcal{G})$ to the Dirichlet region adjacent through this side.

Let $\rho \in T(2,3,8)$ be the rotation around the origin O by $\pi/4$, and let us denote as

$$\mathcal{A} = (a, \overline{b}, c, \overline{d}, \overline{a}, b, \overline{c}, d)$$

the alphabet formed by the generators of $\mathcal{G}$ and their inverses, considered as an ordered sequence (Figure 4). The conjugation by ρ acts as a permutation on $\mathcal{A}$.

The Dirichlet regions for $\mathcal{G}$ have already been studied [25]. The rest of this section is devoted to rephrasing the description in a more intuitive way.

For $x \in \mathcal{A}$, we denote as v_x the vertex of octagon $\mathcal{D}_O(\mathcal{G})$ that is equidistant to O, x, and $\rho^{-1}x\rho$. The eight elements of the alphabet $\mathcal{A}$ are the elements of the orbit $\mathcal{G}O$ that are closest to O. In the same way, the eight elements $xz, z \in \mathcal{A}$ are closest to x. Any $z \in \mathcal{A}$ can be written as $\rho^k\overline{x}\rho^{-k}$, where $0 \leq k < 8$, so, the above $xz, z \in \mathcal{A}$ can be written as $xz = x \cdot \rho^k x \rho^{-k}(O)$.

A careful but straightforward observation of the Dirichlet regions of O, x, $x \cdot \rho\overline{x}\rho^{-1}$, and so on allows to show that:

Observation 8. *Each vertex v_x is incident to eight isometric Dirichlet regions as shown on Figure 6.*

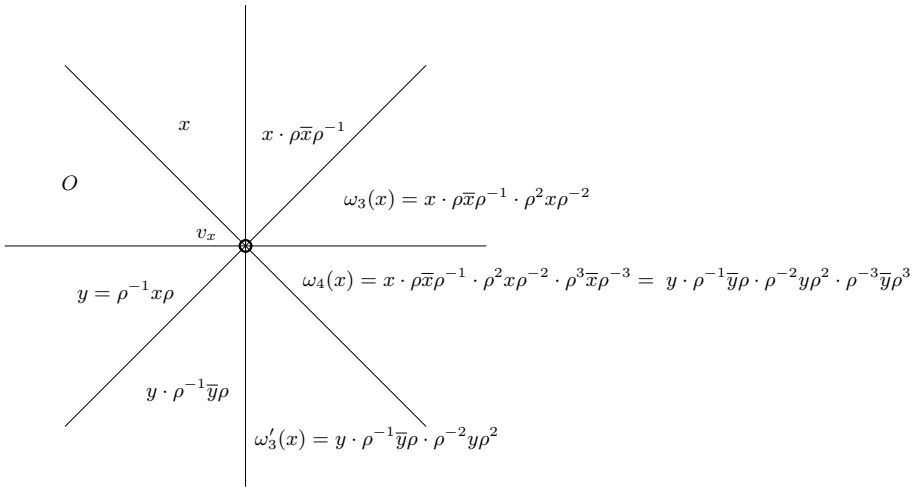

Figure 6: Centers of Dirichlet regions incident to a vertex v_x of $\mathcal{D}_O(\mathcal{G})$

Without loss of generality, we now examine more closely the vertex v of $\mathcal{D}_O(\mathcal{G})$ that is incident to $\mathcal{D}_a(\mathcal{G})$ and $\mathcal{D}_d(\mathcal{G})$ (Figure 4). The eight Dirichlet regions incident to v are centered at the images of O by the following translations, in clockwise order: $F = (\mathbb{1}, a, ab, abc, abcd = dcba, dcb, dc, d)$ (Figure 7).

The eight Dirichlet regions $\rho^k\mathcal{D}_v(\mathcal{G}), 0 \leq k < 8$, share the common vertex O. The Dirichlet region $\mathcal{D}_v(\mathcal{G})$ is isometric to $\mathcal{D}_O(\mathcal{G})$ since v lies in the $T(2,3,8)$-orbit of O; $\mathcal{D}_v(\mathcal{G})$ is the regular octagon with vertices in $F(O)$.

For a point $p \in \mathbb{H}^2$, let $C(p)$ be the set

$$C(p) = \{g \mid g \in \mathcal{G}, \mathcal{D}_p(\mathcal{G}) \cap \mathcal{D}_{g(p)}(\mathcal{G}) \neq \emptyset\}$$

(notation C can be remembered as standing for "crown"). It is easy to check that for $q = t(p), t \in T(2,3,8)$ we have $C(q) = \{tgt^{-1} \mid g \in C(p)\}$.

The dots in Figure 8 show elements of the orbit $T(2,3,8)O$. Let p be a point in triangle SOQ. Let us consider the Dirichlet regions that are adjacent to $\mathcal{D}_p(\mathcal{G})$.

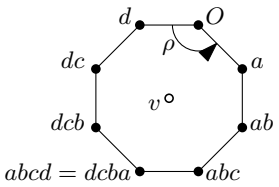

Figure 7: Schematic representation of $\mathcal{D}_v(\mathcal{G})$.

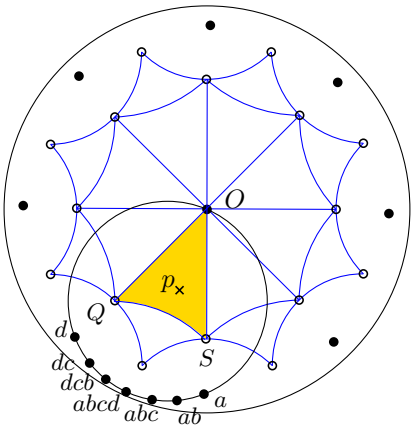

Figure 8: Description of Dirichlet regions.

- If p is in the interior of SQO. The Dirichlet region $\mathcal{D}_p(\mathcal{G})$ is a polygon with 18 sides. Each vertex of $\mathcal{D}_p(\mathcal{G})$ has degree 3. The sides of $\mathcal{D}_p(\mathcal{G})$ have the following labels in counterclockwise order: $a, a\overline{d}, \overline{b}\overline{c}d, \overline{b}, \overline{b}\overline{a}, c, \overline{d}, \overline{a}, b, \overline{c}\overline{d}, \overline{c}, \overline{c}\overline{b}\overline{a}, d\overline{a}, d, dc, dcb, abc, ab$.
- If p lies in the interior of edge OQ, the sides dc and abc degenerate to a vertex of $\mathcal{D}_p(\mathcal{G})$. On SO, the sides ab and dcb degenerate to a vertex, and on QS b and c degenerate to a vertex. Such a new vertex has degree 4. The Dirichlet region $\mathcal{D}_p(\mathcal{G})$ is a polygon with 14 sides.
- When $p \in \{O, Q, S\}$, $\mathcal{D}_p(\mathcal{G})$ degenerates to an octagon (Proposition 7). Its adjacent octagons are centered at points in $C(O), C(Q), C(S)$ respectively.

In particular:

Observation 9. *The Dirichlet region $\mathcal{D}_p(\mathcal{G})$ shares a common vertex with the Dirichlet region $\mathcal{D}_{abcd(p)}(\mathcal{G})$ if and only if p coincides with O.*

Figure 9 was computed using the software described in [6].

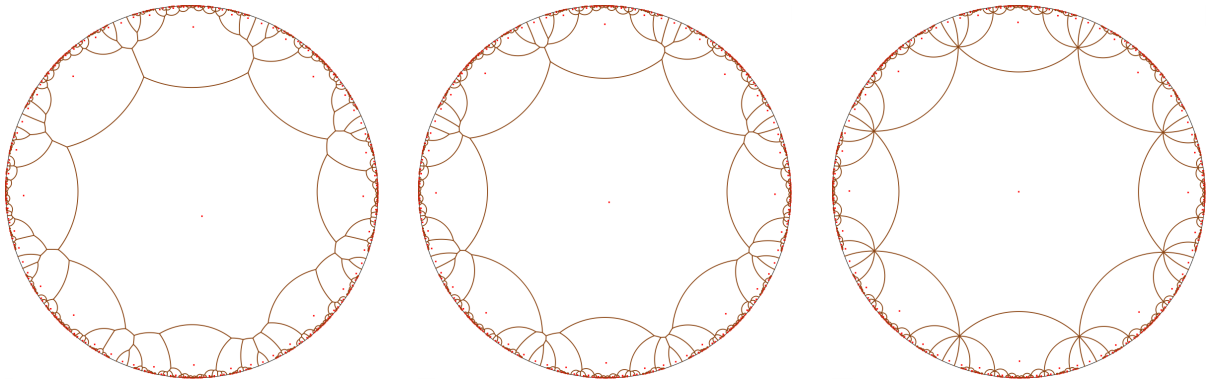

Figure 9: Dirichlet region for $\mathcal{G}$ centered at a point getting closer to O.

Let us define

$$C^-(O) = C(O) \setminus \{\rho^k(abcd)\rho^{-k}(O) \mid 0 \leq k < 8\},$$

i.e. $C^-(O)$ consists of elements of $C(O)$ except $abcd$ and its rotated images around O by powers of ρ. For $O' = rO, r \in T(2,3,8)$, we define $C^-(O') = \{rgr^{-1} \mid g \in C^-(O)\}$. From the description above:

Proposition 10. *For any $p \in \mathbb{H}^2$ there exists $O' \in T(2,3,8)O$, such that $C(p) \subset C(O')$. Moreover, if $p \notin T(2,3,8)O$, then $C(p) \subset C^-(O')$.*

4.2 Short closed geodesics on the Bolza surface

Let us first mention the following result:

Proposition 11. *The largest empty ball diameter for $\mathcal{M}$ satisfies inequality $4.89 < \delta_{\mathcal{M}} < 6.62$.*

Proof. Since the Voronoi cell $\mathcal{D}_O(\mathcal{G})$ is a regular octagon, the radius of the largest ball that does not contain any point of $\mathcal{G}O$ is the distance from O to any vertex of $\mathcal{D}_O(\mathcal{G})$. It can also be seen as the length $l(abcd)$. The origin together with two adjacent vertices of $\mathcal{D}_O(\mathcal{G})$ form a isosceles triangle with angles $\frac{\pi}{4}, \frac{\pi}{8}, \frac{\pi}{8}$. By applying a hyperbolic law of cosines we get that the lateral side of the triangle, which is the radius of the ball, is $acosh(3+2\sqrt{2})$. As a result $\delta_{\mathcal{M}} \geq \delta_O = 2 \cdot acosh(3+2\sqrt{2}) > 4.89$.

The triangle with angles $\frac{\pi}{2}, \frac{\pi}{3}, \frac{\pi}{8}$ shown in Figure 10 is a fundamental domain for $T(2,3,8)$, denoted as $\mathcal{D}_O(T)$. Let p be a point in $\mathbb{H}^2$. δ_p is the diameter of a ball B_p centered at a vertex of $\mathcal{D}_p(\mathcal{G})$ and passing through p. Without loss of generality we can assume that B_p is centered in $\mathcal{D}_O(T)$: otherwise, B_p is centered in some Dirichlet region $t\mathcal{D}_O(T)$ for $T(2,3,8)$, where $t \in T(2,3,8)$, and we consider $q = t^{-1}(p)$ instead of p (by Proposition 7, $\delta_p = \delta_q$ for any $q \in T(2,3,8)p$). Let c denote the center of B_p

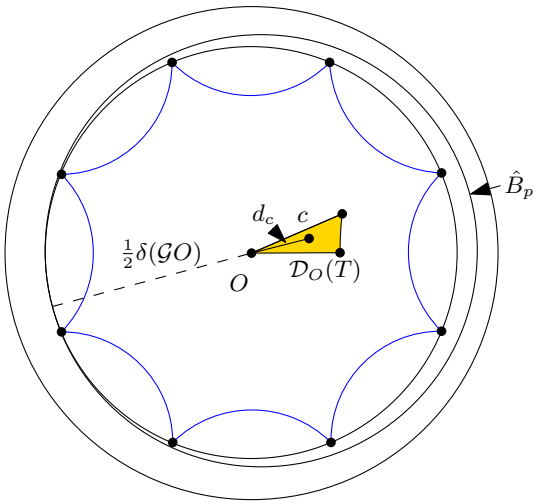

Figure 10: Proof of Proposition 11

and d_c denote the distance from c to O. Let $\hat{B}_p$ be the ball centered at c and of radius $\frac{1}{2}\delta_O + d_c$. This ball contains the ball circumscribing the octagon $\mathcal{D}_O(\mathcal{G})$, whose radius is $\frac{1}{2}\delta_O$, and as a consequence $\hat{B}_p$ contains at least one representative of $\mathcal{G}p$ in its interior. Since both $\hat{B}_p$ and B_p are centered at c, and $\hat{B}_p$ contains a point of $\mathcal{G}p$ while B_p does not contain any, then $\hat{B}_p$ must contain B_p. The diameter of $\hat{B}_p$ is $\delta_O + 2d_c$, so, $\delta_p \leq \delta_O + 2d_c$. To estimate d_c we note that d_c is not greater than the length of the side of $\mathcal{D}_O(T)$ opposite to the vertex with angle $\frac{\pi}{2}$. Calculations using a hyperbolic law of cosines show that $d_c < 0.860707$. So, $\delta_p < 6.62$ for any $p \in \mathbb{H}^2$. □

We can now observe that there are closed geodesics on $\mathcal{M}$ that are shorter than $\delta_{\mathcal{M}}$.

The generators $a, \overline{b}, c, \overline{d}, \overline{a}, b, \overline{c}, d$ of $\mathcal{G}$ are associated with matrices

$$\begin{pmatrix} 1+\sqrt{2} & \exp^{ik\pi/4}\sqrt{2}\sqrt{\sqrt{2}+1} \\ \exp^{-ik\pi/4}\sqrt{2}\sqrt{\sqrt{2}+1} & 1+\sqrt{2} \end{pmatrix}$$

for $k \in \{0, \ldots, 7\}$ respectively, and each element of $\mathcal{G}$ is associated with a product of these matrices. As mentioned in Section 2, the translation length of an element of $\mathcal{G}$ is given by the trace of its matrix.

We just briefly summarize [3]. For the n^{th} element l_n of the length spectrum $L(\mathcal{G})$, $n > 0$, the following holds: $\cosh(l_n/2) = m + n\sqrt{2}$, where for any given n, m is the unique odd natural number minimizing $|m - n\sqrt{2}|$. The authors also compute the multiplicity of each entry in $L(\mathcal{G})$. Table 1 shows the first 30 elements of the length spectrum of $\mathcal{G}$. As can be seen in the table, there are closed geodesics that are shorter than 4.89, thus shorter than $\delta_{\mathcal{M}}$. The second line in the table actually corresponds to closed geodesics whose length is equal to δ_O.

Table 1: A portion of the length spectrum $L(\mathcal{G})$[3].

length	multiplicity	m	n	length	multiplicity	m	n
3.05714183896	24	1	1	9.02707171973	12	23	16
4.89690489536	24	3	2	9.17142551689	72	25	17
5.82807077544	48	5	3	9.22829508964	96	25	18
6.11428367792	24	5	4	9.3592716579	192	27	19
6.67200576991	96	7	5	9.48219414927	48	29	20
7.10737587411	48	9	6	9.53097705714	192	29	21
7.26316347512	48	9	7	9.64406564862	96	31	22
7.59569183041	8	11	8	9.75109975831	336	33	23
7.88069228867	96	13	9	9.79380979071	24	33	24
8.1300755289	48	15	10	9.89331068777	192	35	25
8.22490362326	192	15	11	9.98809463666	192	37	26
8.43684964052	48	17	12	10.0785887303	192	39	27
8.62846365652	96	19	13	10.1149054114	96	39	28
8.70275055643	48	19	14	10.1999558888	384	41	29
8.87147981074	288	21	15	10.2815363765	96	43	30

5 Covering spaces of the Bolza surface

As mentioned at the end of Section 3, we give our own construction of coverings spaces of $\mathcal{M}$ in which, for any set $\mathcal{P}$, the projection $\pi(\mathrm{DT}_{\mathbb{H}}(\Gamma\mathcal{P}))$ does not contain any 1- or 2-cycle.

Let us first illustrate the idea of the construction on the case of the flat (or Euclidean) torus, to give some intuition.

5.1 Back to the Euclidean case

The results in this sections were already presented [7], but the proofs are slightly modified here, so that similarities with the hyperbolic case appear more naturally.

We consider the flat torus $\mathcal{T}_1 = \mathbb{E}^2/\mathcal{G}_1^{\mathbb{E}}$, where $\mathcal{G}_1^{\mathbb{E}}$ is the (commutative) group generated by two translations t_x and t_y of the same length l along the axes of $\mathbb{E}^2$. Since $\mathcal{G}_1^{\mathbb{E}}$ is Abelian, any $x \in \mathcal{G}_1^{\mathbb{E}}$ can be uniquely written as $x = t_x^{\alpha} t_y^{\beta}$, where $\alpha, \beta \in \mathbb{Z}$. The *size* $\lambda_1(x)$ of x can be defined as the sum $|\alpha| + |\beta|$.

The Dirichlet region for $\mathcal{G}_1^{\mathbb{E}}$ centered at any point in $\mathbb{E}^2$ is a square of edge length l. It is easy to see that the systole of $\mathcal{T}_1$ is equal to l, and that the largest empty disk diameter $\delta_{\mathcal{G}_1^{\mathbb{E}}}$ is $\sqrt{2}l$. We denote the Dirichlet region for $\mathcal{G}_1^{\mathbb{E}}$ centered at the origin point O by $\mathcal{D}_1$.

Similarly as done for the hyperbolic case, in the sequel the inverse of a translation x of $\mathcal{G}_1^{\mathbb{E}}$ will be denoted as $\overline{x}$. For simplicity, x both denotes an element x of $\mathcal{G}_1^{\mathbb{E}}$ and the image $x(O)$ of the origin O by x.

The group $\mathcal{G}_1^{\mathbb{E}}$ is Abelian, so, all its subgroups are normal. Let us consider the subgroup $\mathcal{G}_2^{\mathbb{E}}$ consisting of elements of $\mathcal{G}_1^{\mathbb{E}}$ of even size. It is easy to see that $\mathcal{G}_2^{\mathbb{E}} = \langle \overline{t_x} t_y, t_x t_y \rangle$.

Lemma 12. *$\mathcal{G}_2^{\mathbb{E}}$ is a subgroup of index 2 in $\mathcal{G}_1^{\mathbb{E}}$.*

Proof. Let $\varphi : \mathcal{G}_1^{\mathbb{E}} \to \mathbb{Z}_2$ be the group homomorphism

$$\begin{array}{rccc} \varphi : & \mathcal{G}_1^{\mathbb{E}} & \to & \mathbb{Z}_2 \\ & x & \mapsto & \lambda_1(x) \mod 2 \end{array}$$

The subgroup $\mathcal{G}_2^{\mathbb{E}}$ is the kernel of φ, and the image of φ is $\mathbb{Z}_2$. According to the First Isomorphism Theorem (see, e.g., [2]) $\ker\varphi$ is a normal subgroup of $\mathcal{G}_1^{\mathbb{E}}$ (which is trivial here since $\mathcal{G}_1^{\mathbb{E}}$ is Abelian), and $\mathcal{G}_1^{\mathbb{E}}/\ker\varphi \cong \phi(\mathcal{G}_1^{\mathbb{E}})$. Therefore, $\mathcal{G}_1^{\mathbb{E}}/\mathcal{G}_2^{\mathbb{E}} \cong \mathbb{Z}_2$. □

For any $k > 0$, if $\mathcal{G}_{2^{k-1}}^{\mathbb{E}}$ is a subgroup of index 2^{k-1} of $\mathcal{G}_1^{\mathbb{E}}$ generated by two elements, i.e., $\mathcal{G}_{2^{k-1}}^{\mathbb{E}} = \langle g, h\rangle\ ,\ g, h \in \mathcal{G}_1^{\mathbb{E}}$, we construct the subgroup $\mathcal{G}_{2^k}^{\mathbb{E}}$ of $\mathcal{G}_{2^{k-1}}^{\mathbb{E}}$ as follows: $\mathcal{G}_{2^k}^{\mathbb{E}} = \langle \overline{g}h, gh\rangle$. The proof of the following lemma is similar to that of Lemma 12.

Lemma 13. *For any $k > 0$, $\mathcal{G}_{2^k}^{\mathbb{E}}$ is a subgroup of index 2^k in $\mathcal{G}_1^{\mathbb{E}}$.*

By construction, for any $k \geq 0$, the generators of $\mathcal{G}_{2^k}^{\mathbb{E}}$ are two translations whose vectors are orthogonal and of equal length $\sqrt{2}^k l$. The orbits of $\mathcal{G}_{2^k}^{\mathbb{E}}$ are isomorphic to $\mathbb{Z}^2$ and the Dirichlet region $\mathcal{D}_{2^k}$ for $\mathcal{G}_{2^k}^{\mathbb{E}}$ centered at O is a square of edge length $\sqrt{2}^k l$ (See Figure 11).

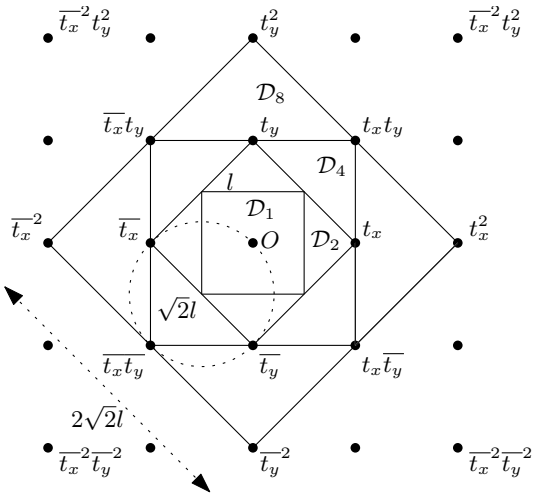

Figure 11: Euclidean case.

For any $k > 0$, $\mathcal{T}_{2^k} = \mathbb{E}^2/\mathcal{G}_{2^k}^{\mathbb{E}}$ is a flat torus, with the corresponding projection map $\pi_{2^k} : \mathbb{E}^2 \to \mathcal{T}_{2^k}$. The systole $sys(\mathcal{T}_{2^k})$ of $\mathcal{T}_{2^k}$ is equal to $\sqrt{2}^k l$. The torus $\mathcal{T}_{2^k}$ is a covering space of $\mathcal{T}_1$ with covering map $\rho_k := \pi_1 \circ \pi_{2^k}^{-1}$. Since the index of $\mathcal{G}_{2^k}^{\mathbb{E}}$ in $\mathcal{G}_1^{\mathbb{E}}$ is 2^k, we get the following result:

Proposition 14. *For any $k > 0$, $\mathcal{T}_{2^k}$ is a 2^k-sheeted covering space of $\mathcal{T}_1$.*

Let $\delta(\mathcal{P})$ denote the diameter of the largest disk in $\mathbb{E}^2$ that does not contain any point of a set $\mathcal{P}$ in its interior. Note that for any $p \in \mathbb{E}^2, \delta(\mathcal{G}_{2^k}^{\mathbb{E}} p) = \sqrt{2}^{k+1} l$.

The following is the analog of Proposition 4:

Proposition 15. *For a flat torus $\mathcal{T} = \mathbb{E}^2/\mathcal{G}^{\mathbb{E}}$ and a set of points $\mathcal{P}$,*
(1) if $sys(\mathcal{T}) > \delta(\mathcal{G}^{\mathbb{E}}\mathcal{P})$, then the graph of edges of $\pi(DT_{\mathbb{E}}(\mathcal{G}^{\mathbb{E}}\mathcal{P}))$ has no 1-cycle.
(2) if $sys(\mathcal{T}) > 2\delta(\mathcal{G}^{\mathbb{E}}\mathcal{P})$, then the graph of edges of $\pi(DT_{\mathbb{E}}(\mathcal{G}^{\mathbb{E}}\mathcal{P}))$ has no 2-cycle.

Then, from Propositions 14 and 15, we get:

Proposition 16. *For any $\mathcal{P}$,*
(1) if $sys(\mathcal{T}_{2^k}) > \delta(\mathcal{G}_1^{\mathbb{E}}\mathcal{P})$, then $\pi_{2^k}(DT_{\mathbb{E}}(\mathcal{G}_1^{\mathbb{E}}\mathcal{P}))$ has no 1-cycle,
(2) if $sys(\mathcal{T}_{2^k}) > 2\delta(\mathcal{G}_1^{\mathbb{E}}\mathcal{P})$, then $\pi_{2^k}(DT_{\mathbb{E}}(\mathcal{G}_1^{\mathbb{E}}\mathcal{P}))$ has no 2-cycle, for any $\mathcal{P}$.

Corollary 17. *For any $\mathcal{P}$,*
(1) the graph of edges of the projection $\pi_4(DT_{\mathbb{E}}(\mathcal{G}_1^{\mathbb{E}}\mathcal{P}))$ of $DT_{\mathbb{E}}(\mathcal{G}_1^{\mathbb{E}}\mathcal{P})$ onto $\mathcal{T}_4$ has no 1-cycle,
(2) the graph of edges of the projection of $DT_{\mathbb{E}}(\mathcal{G}_1^{\mathbb{E}}\mathcal{P})$ onto $\mathcal{T}_{16}$ (and a fortiori *onto any $\mathcal{T}_{2^k}$ for $k \geq 4$) has no 2-cycle.*

For $\mathcal{T}_8$, we have exactly $sys(\mathcal{T}_8) = 2\delta_{\mathcal{T}}$, so, the above criteria do not directly allow us to conclude. Still, we show that:

Proposition 18. *If $\mathcal{P} \subset \mathbb{E}^2$ contains at least two distinct points that do not lie on the same $\mathcal{G}_1^{\mathbb{E}}$-orbit, then the graph of edges of the projection $\pi_8(DT(\mathcal{G}_1^{\mathbb{E}}\mathcal{P}))$ onto $\mathcal{T}_8$ has no 2-cycle.*

Proof. The maximum empty disk diameter $\delta(\mathcal{G}_1^{\mathbb{E}}p)$, for any $p \in \mathcal{P}$, is $\sqrt{2}l = \frac{1}{2}\delta(\mathcal{G}_8^{\mathbb{E}})$ (Figure 11). Let us show that $\delta(\mathcal{G}_1^{\mathbb{E}}\mathcal{P})$ is strictly less than $\sqrt{2}l$. Let $\mathcal{B}_{\sqrt{2}}$ be a disk of diameter $\sqrt{2}l$ centered at some point $c \in \mathbb{E}^2$ and containing no point of $\mathcal{G}_1^{\mathbb{E}}\mathcal{P}$ in its interior. The disk $\mathcal{B}_{\sqrt{2}}$ contains the Dirichlet region $\mathcal{D}_1(c)$ for $\mathcal{G}_1^{\mathbb{E}}$ centered at c. The four vertices of $\mathcal{D}_1(c)$, which are all on the same $\mathcal{G}_1^{\mathbb{E}}$-orbit, lie on the boundary of $\mathcal{B}_{\sqrt{2}}$. For $p, q \in \mathcal{P}, q \notin \mathcal{G}_1^{\mathbb{E}}p$, there is a representative of $\mathcal{G}_1^{\mathbb{E}}p$ and a representative of $\mathcal{G}_1^{\mathbb{E}}q$ in $\mathcal{D}_1(c)$. At least one of these representatives lies in the interior of $\mathcal{B}_{\sqrt{2}}$. So, the interior of $\mathcal{B}_{\sqrt{2}}$ is not empty.

If we add more points, the diameter of the largest empty disk cannot become larger. By Proposition 16, the graph of edges of $\pi_8(DT(\mathcal{G}_1^{\mathbb{E}}\mathcal{P}))$ has no 2-cycle. □

In Section 5.3, we construct covering spaces of the Bolza surface in a similar spirit: we look for subgroups of $\mathcal{G}$ whose associated Dirichlet regions keep some symmetry. Let us first mention some properties of such subgroups of $\mathcal{G}$.

5.2 Subgroups of $\mathcal{G}$ and triangle groups

There are three triangle groups $T(2,3,8), T(2,4,8), T(2,8,8)$ for which $\mathcal{G}$ is a normal subgroup. They all contain the rotation ρ, already defined above, and the reflection τ with respect to the axis X_a of translation a. For now on, $\widetilde{\mathcal{G}}$ denotes a subgroup of $\mathcal{G}$. Obviously, if $\widetilde{\mathcal{G}}$ is a normal subgroup of one of these three triangle groups, then $\widetilde{\mathcal{G}} = \rho\widetilde{\mathcal{G}}\rho^{-1}, \widetilde{\mathcal{G}} = \tau\widetilde{\mathcal{G}}\tau^{-1}$.

Let us introduce $N_O(\widetilde{\mathcal{G}})$ defined as the subset of elements $g \in \widetilde{\mathcal{G}}$ such that the Dirichlet regions $\mathcal{D}_O(\widetilde{\mathcal{G}})$ and $\mathcal{D}_g(\widetilde{\mathcal{G}})$ are adjacent (i.e., they share a common edge). For $\widetilde{\mathcal{G}} = \mathcal{G}$, $N_O(\mathcal{G}) = \mathcal{A}$. More generally, $N_O(\widetilde{\mathcal{G}})$ generates $\widetilde{\mathcal{G}}$ [22].

Observation 19. *The Dirichlet region $\mathcal{D}_O(\widetilde{\mathcal{G}})$ for $\widetilde{\mathcal{G}}$ centered at O is invariant by ρ (resp. τ) if and only if $\widetilde{\mathcal{G}} = \rho\widetilde{\mathcal{G}}\rho^{-1}$ (resp. $\widetilde{\mathcal{G}} = \tau\widetilde{\mathcal{G}}\tau^{-1}$).*

Proof. If $\widetilde{\mathcal{G}} = \rho\widetilde{\mathcal{G}}\rho^{-1}$, then the set $\widetilde{\mathcal{G}}O$ maps onto itself under ρ: $\rho\widetilde{\mathcal{G}}O = \rho\widetilde{\mathcal{G}}\rho^{-1}O = \widetilde{\mathcal{G}}O$. Thus the Dirichlet region $\mathcal{D}_O(\widetilde{\mathcal{G}})$, as a Voronoi cell in $\mathrm{VD}_{\mathbb{H}}(\widetilde{\mathcal{G}}O)$, remains invariant under ρ. Similarly it remains invariant under τ.

Now assume that $\mathcal{D}_O(\widetilde{\mathcal{G}})$ is invariant under ρ. Then in particular the sets $N_O(\widetilde{\mathcal{G}})(O)$ and $\rho N_O(\widetilde{\mathcal{G}})(O)$ are equal. If we rewrite $\rho N_O(\widetilde{\mathcal{G}})(O)$ as $\rho N_O(\widetilde{\mathcal{G}})\rho^{-1}(O)$, then $N_O(\widetilde{\mathcal{G}})(O) = \rho N_O(\widetilde{\mathcal{G}})\rho^{-1}(O)$. So, for all $g \in N_O(\widetilde{\mathcal{G}})$, there is some $h \in N_O(\widetilde{\mathcal{G}})$ such that $g(O) = \rho h\rho^{-1}(O)$. Since $\mathcal{G} = \rho\mathcal{G}\rho^{-1}$, then $\rho h\rho^{-1}$ is in $\mathcal{G}$. Thus the translation $\rho h\rho^{-1} \cdot \overline{g}$ is in $\mathcal{G}$, and it maps O onto itself. Since $\mathcal{G}$ has no fixed point, it must be the identity. So, $\rho h\rho^{-1} = g$. This is true for all g in $N_O(\widetilde{\mathcal{G}})$, and as a consequence $N_O(\widetilde{\mathcal{G}}) = \rho N_O(\widetilde{\mathcal{G}})\rho^{-1}$. Since the elements of $N_O(\widetilde{\mathcal{G}})$ generate $\widetilde{\mathcal{G}}$, the elements of $\rho N_O(\widetilde{\mathcal{G}})\rho^{-1}$ generate $\rho\widetilde{\mathcal{G}}\rho^{-1}$. Since $N_O(\widetilde{\mathcal{G}}) = \rho N_O(\widetilde{\mathcal{G}})\rho^{-1}$, we have $\widetilde{\mathcal{G}} = \rho\widetilde{\mathcal{G}}\rho^{-1}$.

The same proof works for τ as well (the only property of ρ that we used is that $\rho(O) = O$, which is also true for τ. □

We get the following result as a corollary of the last observation.

Proposition 20. *If $\widetilde{\mathcal{G}}$ is normal in a triangle reflection group, then $\mathcal{D}_O(\widetilde{\mathcal{G}})$ is invariant under ρ and τ.*

The triangle groups mentioned above are of the form $T(2,m,n)$, they can be generated by ρ, τ and some additional rotation r_{mn}. If the Dirichlet region $\mathcal{D}_O(\widetilde{\mathcal{G}})$ is invariant under ρ and τ, then $\widetilde{\mathcal{G}}$ is normal in $T(2,m,n)$ if and only if $\widetilde{\mathcal{G}} = r_{mn}\widetilde{\mathcal{G}}r_{mn}^{-1}$.

5.3 Covering space for which the projection of $\mathrm{DT}_{\mathbb{H}}(\mathcal{GP})$ has no 1-cycle

Before explicitly constructing subgroups of $\mathcal{G}$, let us prove the following property:

Proposition 21. *The condition that $\widetilde{\mathcal{G}}$ contains no element of $C^-(O')$ for any $O' \in T(2,3,8)O$ is necessary and sufficient for the graph of edges of the projection of $DT_{\mathbb{H}}(\mathcal{GP})$ onto $\widetilde{\mathcal{M}} = \mathbb{H}^2/\widetilde{\mathcal{G}}$ to have no 1-cycle, for any $\mathcal{P}$.*

Proof. Let e be an edge of $DT_{\mathbb{H}}(\mathcal{GP})$, such that $\pi(e)$ is a geodesic loop on $\mathcal{M}$, i.e., the endpoints of e are p and $g(p)$ for some $p \in \mathbb{H}^2$ and $g \in \mathcal{G}$. Then g is in $C(p)$: indeed, since $e \in DT_{\mathbb{H}}(\mathcal{GP})$, the Voronoi cells $V_p(\mathcal{GP})$ and $V_{g(p)}(\mathcal{GP})$ have a common point. Note that $V_p(\mathcal{GP}) \subset V_p(\mathcal{G}p) = \mathcal{D}_p(\mathcal{G})$, and similarly $V_{g(p)}(\mathcal{GP}) \subset \mathcal{D}_{g(p)}(\mathcal{G})$. Then $\mathcal{D}_p(\mathcal{G}) \cap \mathcal{D}_{g(p)}(\mathcal{G}) \neq \emptyset$, i.e., $g \in C(p)$.

By Proposition 10, $g \in C(p) \subset C(O')$ for some $O' \in T(2,3,8)O$. So, if $\widetilde{\mathcal{G}}$ is a subgroup of $\mathcal{G}$ that contains no elements of $C(O')$, then the projection of $DT_{\mathbb{H}}(\mathcal{GP})$ to $\widetilde{\mathcal{M}} = \mathbb{H}^2/\widetilde{\mathcal{G}}$ has no 1-cycle. Now let us show that $g \in C^-(O')$. Assume that $g \in C(p)$ is in $C(O')$, but not in $C^-(O')$. Then Proposition 10 implies that $p \in T(2,3,8)O$. Without loss of generality assume $p = O$ and $g = abcd$. If $\mathcal{P}$ contains more than one point, then the triangulation cannot have an edge incident to O and $abcd$. If $\mathcal{P} = \{O\}$, then as shown on Figure 12, we can choose[2] a triangulation of the octagon $\mathcal{D}_v(\mathcal{G})$ in $\mathbb{H}^2$ that does not have an edge incident to O and $abcd$. Then the projection of $DT_{\mathbb{H}}(\mathcal{GP})$ has no 1-cycle. Remark that for any

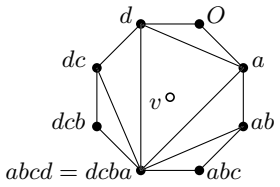

Figure 12: Proof of Proposition 21: avoiding edge with vertices O and $abdc$.

$g \in C^-(O)$, we can choose $DT_{\mathbb{H}}(\mathcal{G}O)$ so that the geodesic segment with endpoints O and g is an edge of $DT_{\mathbb{H}}(\mathcal{G}O)$. The result follows. □

The rest of this section sketches the construction of small index subgroups of $\mathcal{G}$.

In the sequel, we use the standard notation $[g,h]$ for the *commutator* of two isometries g and h, i.e., $[g,h] = ghg^{-1}h^{-1}$. The generators of $\mathcal{G}_2$, in the form given in Proposition 22, are $x \cdot \rho\overline{x}\rho^{-1} = [x,\rho]$.

Subgroup $\mathcal{G}_2$

We first define the subgroup $\mathcal{G}_2$ of $\mathcal{G}$ generated by words of even size in the alphabet $\mathcal{A}$ (Figure 13).

The proof of Lemma 12 is actually general, and it allows to show that $\mathcal{G}_2$ is a subgroup of index 2 in $\mathcal{G}$. Hence, $\mathcal{G}_2$ is normal in $\mathcal{G}$.

We can describe the generators of $\mathcal{G}_2$ as follows.

Proposition 22. *$\mathcal{G}_2$ is generated by $\{x \cdot \rho\overline{x}\rho^{-1} = [x,\rho] \mid x \in \mathcal{A}\}$.*

Proof. It is sufficient to prove that any word of size 2 on $\mathcal{A}$ can be generated by this subset. Let us take word $yz \in \mathcal{G}_2$, where $y, z \in \mathcal{A}$. As mentioned in Section 4, ρ acts as a permutation on $\mathcal{A}$, i.e., we can write $y = \rho^{k_1}x\rho^{-k_1}$ and $z = \rho^{k_2}\overline{x}\rho^{-k_2}$ for some $k_1, k_2, 0 \leq k_1, k_2 < 8$. Then yz can be written as $yz = (\rho^{k_1}x\rho^{-k_1} \cdot \rho^{k_1+1}\overline{x}\rho^{-k_1-1}) \cdot (\rho^{k_1+1}x\rho^{-k_1-1} \cdot \rho^{k_1+2}\overline{x}\rho^{-k_1-2}) \cdot \ldots \cdot (\rho^{k_2-1}x\rho^{-k_2+1} \cdot \rho^{k_2}\overline{x}\rho^{-k_2})$. □

The subgroup $\mathcal{G}_2$ can be written in a finitely presented form:

$$\mathcal{G}_2 = \left\langle ab, cd, \overline{a}\overline{b}, \overline{c}\overline{d}, bc, d\overline{a}, \overline{b}\overline{c}, \overline{d}a \mid abcd\overline{a}\overline{b}\overline{c}\overline{d} \right\rangle.$$

As a consequence of Observation 8, $[x,\rho]$, $[\rho^{-1}x\rho,\rho]$ and O are equidistant to v_x, and the Dirichlet region of O for $\mathcal{G}_2$ can be completely described (See Figure 13):

Observation 23. *The fundamental region $\mathcal{D}_O(\mathcal{G}_2)$ has 16 vertices that form the circular sequence $(v_x,\ x \mid x \in \mathcal{A})$, in counterclockwise order.*
The set $N_O(\mathcal{G}_2)$ is the circular sequence of translations $([x,\rho],[x,\rho^{-1}] \mid x \in \mathcal{A})$ in counterclockwise order.

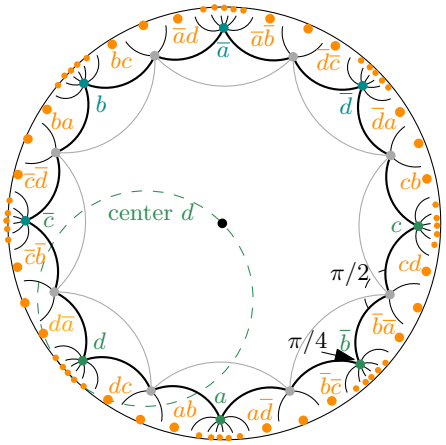

Figure 13: Dirichlet region for $\mathcal{G}_2$.

The Dirichlet region of O is clearly invariant under ρ and τ. Indeed, since conjugation by ρ or τ leaves $\mathcal{A}$ invariant, it preserves the size of a word in $\mathcal{G}$. As a consequence, by Observation 19, $\mathcal{G}_2 = \rho\mathcal{G}_2\rho^{-1} = \tau\mathcal{G}_2\tau^{-1}$.

We can actually show that:

Proposition 24. *$\mathcal{G}_2$ is the only subgroup of index 2 of $\mathcal{G}$ for which the Dirichlet region centered at O is invariant by ρ.*

Proof. Let $\mathcal{G}'_2$ be another subgroup of $\mathcal{G}$ satisfying these properties. We first remark that if there is some element of $\mathcal{A}$ that is in $\mathcal{G}'_2$, then from the symmetry property with respect to ρ, and the fact that conjugation by ρ acts as a permutation in $\mathcal{A}$, then all elements of $\mathcal{A}$ are in $\mathcal{G}'_2$, and $\mathcal{G}'_2 = \mathcal{G}$. So, $\mathcal{G}'_2$ does not contain any element of $\mathcal{A}$.

Let us now assume that there exist $x, y \in \mathcal{A}$ such that $xy \notin \mathcal{G}'_2$. Since $\mathcal{G}'_2$ is a subgroup of index 2 of $\mathcal{G}$, $\mathcal{G}$ can be written as a disjoint union of cosets as $\mathcal{G} = \mathcal{G}'_2 \cup \mathcal{G}'_2xy$. Also, since $y \notin \mathcal{G}'_2$, $\mathcal{G} = \mathcal{G}'_2 \cup \mathcal{G}'_2y$. Then we would have $\mathcal{G}_2 = \mathcal{G}_2x$, i.e., $x \in \mathcal{G}'_2$. This is a contradiction, showing that all elements of size 2 on alphabet $\mathcal{A}$ belong to $\mathcal{G}'_2$. So, $\mathcal{G}'_2 = \mathcal{G}_2$. □

The generators of $\mathcal{G}_2$ all have the same translation length, it is actually equal to the translation length of a, b, c, d (this can easily be computed from their matrices). As a result, the hyperbolic surface $\mathcal{M}_2 = \mathbb{H}^2/\mathcal{G}_2$ still contains shortest loops of length $sys(\mathcal{M})$ (i.e. $sys(\mathcal{M}_2) = sys(\mathcal{M})$). There are fewer shortest loops than on $\mathcal{M}$, since the elements of $\mathcal{A}$ are not in $\mathcal{G}_2$.

Subgroup G_4

We now define $\mathcal{G}_4$ to be generated by words of even size in the alphabet of generators of $\mathcal{G}_2$. For $x \in \mathcal{A}$, let $\omega_4(x)$ denote the element $x \cdot \rho\overline{x}\rho^{-1} \cdot \rho^2 x\rho^{-2} \cdot \rho^3\overline{x}\rho^{-3}$ (See Figure 6).

Observation 25. *The fundamental region $\mathcal{D}_O(\mathcal{G}_4)$ has 24 vertices that form the circular sequence $([x,\rho], x, [x,\rho^{-1}] \mid x \in \mathcal{A})$, in counterclockwise order.*
The set $N_O(\mathcal{G}_4)$ is the circular sequence $(\omega_4(x), x \cdot \rho^2\overline{x}\rho^{-2}, x \cdot \rho^{-2}\overline{x}\rho^2 \mid x \in \mathcal{A})$, in counterclockwise order.

Proof. Let Π be the polygon with vertices $([x,\rho], x, [x,\rho^{-1}] \mid x \in \mathcal{A})$, in counterclockwise order. Consider a vertex $x \in \mathcal{A}$ of Π. Recall that the elements of the set $\{x \cdot \rho^k\overline{x}\rho^{-k} \mid 0 \le k < 8\}$ are equidistant from x. In particular, $x \cdot \rho^2\overline{x}\rho^{-2}$ and $x \cdot \rho^{-2}\overline{x}\rho^2$ are equidistant from x.

Note that $(\rho \cdot x \cdot \rho^{-1}) \cdot (\rho^2 \cdot \overline{x} \cdot \rho^{-2})$, $(\rho^2 \cdot x \cdot \rho^{-2}) \cdot (\rho^3 \cdot \overline{x} \cdot \rho^{-3})$, and $\rho\overline{x}\rho^{-1} \cdot \overline{x}$ are vertices of $\mathcal{D}_O(\mathcal{G}_2)$ equidistant to O. Thus $[x,\rho] \cdot (\rho \cdot x \cdot \rho^{-1}) \cdot (\rho^2 \cdot \overline{x} \cdot \rho^{-2})$, $[x,\rho] \cdot (\rho^2 \cdot x \cdot \rho^{-2}) \cdot (\rho^3 \cdot \overline{x} \cdot \rho^{-3})$, and $[x,\rho]\rho\overline{x}\rho^{-1} \cdot \overline{x}$ are equidistant from the vertex $[x,\rho]$ of Π, i.e., $x \cdot \rho^2\overline{x}\rho^{-2}$, $\omega_4(x)$, and O are equidistant from the vertex $[x,\rho]$ of Π. The proof is similar for the vertex $[x,\rho^{-1}]$. □

As a corollary, using the fact that $N_O(\mathcal{G}_4)$ generates $\mathcal{G}_4$, we get:

[2] see also the treatment of degenerate cases at the beginning of Section 3

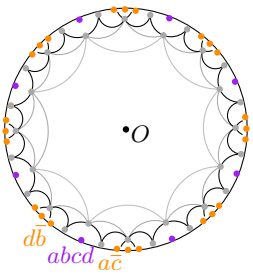

Figure 14: Dirichlet region for $\mathcal{G}_4$.

Corollary 26. *The set* $\{\omega_4(x), x \cdot \rho^2\overline{x}\rho^{-2}, x \cdot \rho^{-2}\overline{x}\rho^2 \mid x \in \mathcal{A}\}$ *generates* $\mathcal{G}_4$.

In other words, the generators of $\mathcal{G}_4$ are $ac, abcd, d\bar{b}$, and their conjugates by $\rho^k, 1 < k < 8$ (Figure 14).

In a similar way as done for $\mathcal{G}_2$, we can show that $\mathcal{G}_4$ is the only subgroup of index 2 of $\mathcal{G}_2$ for which the Dirichlet region centered at O is invariant by ρ.

Proposition 27. *The systole of* $\mathcal{M}_4 = \mathbb{H}^2/\mathcal{G}_4$ *is equal to the translation length of* $abcd$.

Proof. The systole $sys(\mathcal{M})$ is equal to the translation length $l(a)$ of the translation a. The translations of $\mathcal{G}$ that have the same translation length as a are conjugates hah^{-1}, where $h \in T(2,3,8)$. As $a \notin \mathcal{G}_4$ and $\mathcal{G}_4$ is normal in $T(2,3,8)$, it does not contain hah^{-1} for any $h \in T(2,3,8)$. Thus $sys(\mathbb{H}^2/\mathcal{G}_4)$ is greater than $l(a)$.

The second line in the length spectrum of $\mathbb{H}^2/\mathcal{G}$ (Table 1) corresponds to geodesics of length $l(abcd)$ (showing that $l(abcd) = 2 \cdot acosh(3 + 2\sqrt{2})$ is only technical work, omitted here). Since $abcd \in \mathcal{G}_4$ (it corresponds to a violet point $abcd(O)$ in Figure 14), the result follows. □

The systole of $\mathcal{M}_4$ is greater than $sys(\mathcal{M})$, but still smaller than $\delta_{\mathcal{M}}$. However, as a consequence of Proposition 21:

Proposition 28. *For any* $\mathcal{P}$, *the projection of* $DT_{\mathbb{H}}(\mathcal{GP})$ *on* $\mathcal{M}_4$ *has no 1-cycle.*

5.4 Covering space for which the projection of $\mathrm{DT}_{\mathbb{H}}(\mathcal{GP})$ has no 2-cycle

The following proposition motivates resorting to an automatic procedure:

Proposition 29. *The index of a subgroup* $\widetilde{\mathcal{G}}$ *for which* $sys(\mathbb{H}^2/\widetilde{\mathcal{G}}) > 2\delta_{\mathcal{M}}$ *is greater than* 32.

Proof. Let $\widetilde{M} = \mathbb{H}^2/\widetilde{\mathcal{G}}$ be a covering space of $\mathcal{M}$ for which $sys(\mathbb{H}^2/\widetilde{\mathcal{G}}) > 2\delta_{\mathcal{M}}$. We construct a lower bound on the area of $\widetilde{M}$. Let D be a maximal disk in $\widetilde{M}$ (i.e., a disk that does not "overlap"). It can be thought as the maximal inscribed disk in some Dirichlet region for $\widetilde{\mathcal{G}}$, so, the diameter of D is equal to $sys(\widetilde{M})$. The area of D is $Area(D) = 2\pi(\cosh R - 1)$, where R is the radius of D, so, if $sys(\widetilde{M}) > 2\delta_{\mathcal{M}}$, then $Area(D) > 2\pi(\cosh \delta_{\mathcal{M}} - 1)$. Moreover, clearly, $Area(\widetilde{M}) > Area(D)$. Thus, $Area(\widetilde{M}) > 2\pi(\cosh \delta_{\mathcal{M}} - 1)$.

The area $Area(\mathcal{M})$ is 4π. So, $Area(\widetilde{M})/Area(\mathcal{M}) > (\cosh \delta_{\mathcal{M}} - 1)/2 > 32.9704$, using the lower bound in Proposition 11. Therefore $\widetilde{M}$ consists of more than 32 sheets of $\mathcal{M}$. □

Following Section 3, we are looking for a normal subgroup $\widetilde{\mathcal{G}}$ of $\mathcal{G}$ that contains

- no product of two elements forming a simple closed geodesic on $\mathcal{M}$ corresponding to a conjugacy class that appears in the portion of the length spectrum $L|_{2\delta_{\mathcal{M}}} = \{l \in L(\mathcal{G}), l \leq 2\delta_{\mathcal{M}}\}$ —we call $\mathcal{L}_0$ the list of these elements,
- no element of conjugacy classes that correspond to unions of two non intersecting 1-cycles on $\mathcal{M}$ sharing their vertex —we call $\mathcal{L}_\cup$ the list of these elements.

In the sequel, we first show how to compute $\mathcal{L}_0$, then $\mathcal{L}_\cup$, and we finally show how to find a group not containing their elements. More precisely, we will find a group that contains one of their elements, but still gives a covering space in which the projection of $\mathrm{DT}_{\mathbb{H}}(\mathcal{GP})$ has no 2-cycle.

$\mathcal{L}_0$ — 2-cycles as simple closed geodesics.
We propose an approach for computing the number of self-intersections of a closed geodesic γ corresponding to a conjugacy class $[g], g \in \mathcal{G}$, in $\mathcal{G}$. As a consequence, this allows us to compute a portion of the length spectrum $L_i(\mathcal{G}), i > 0$ consisting of closed geodesics that have at most i transversal self-intersections. Due to lack of space, we present a simplified version that only allows us to check whether a closed geodesic is simple, which is actually all we need here.

If g is non-primitive, then $g = \hat{g}^n$ for some primitive $\hat{g} \in \mathcal{G}$ and $n > 1$, the number of transversal self-intersections of γ is n times the number of transversal self-intersections of $\hat{\gamma}$. So, for our purpose, we can assume that g is primitive.

In [3] the authors compute a portion of $L(\mathcal{G})$, together with one representative for each conjugacy class (Table 1). They show that the axis of each obtained representative intersects the Dirichlet region $\mathcal{D}_O(\mathcal{G})$, so, $X_g \cap \mathcal{D}_O(\mathcal{G}) \neq \emptyset$. The closed geodesic γ has a transversal self-intersection p *iff* there exist distinct $g_1, g_2 \in [g]$ whose axes X_{g_1}, X_{g_2} intersect in a lift $\tilde{p} \in \pi^{-1}(p)$ [26]. Recall that $X_{hg\overline{h}} = hX_g$ for any $h \in \mathcal{G}$. If h sends $\tilde{p}$ to $\mathcal{D}_O(\mathcal{G})$, then $X_{hg_1\overline{h}}$ and $X_{hg_2\overline{h}}$ intersect in $\mathcal{D}_O(\mathcal{G})$. Thus we consider only the axes that intersect in $\mathcal{D}_O(\mathcal{G})$.

The method is as follows: We first compute $[g]_O = \{g' \in [g] \mid X_{g'} \cap \mathcal{D}_O(\mathcal{G}) \neq \emptyset\}$. Proposition 30 shows that $[g]_O$ is finite. Then we check for pairwise intersections in $\mathcal{D}_O(\mathcal{G})$ between these axes.

Proposition 30. *$[g]_O$ is finite.*

Proof. We take a segment $[p, g(p)]$ of the axis X_g. The segment $[p, g(p)]$ is covered by a finite subset of $\{\mathcal{D}_x(\mathcal{G}) \mid x \in \mathcal{G}O\}$, since $\mathcal{G}$ is discrete and the segment is compact. Denote the Dirichlet regions that intersect $[p, g(p)]$ by $\mathcal{D}_i, i \in \{1, \ldots, m+1\}$, in the order in which they are traversed by X_g from p to $g(p)$ (See Figure 15). Since $p \in \mathcal{D}_1$, then $g(p) \in g\mathcal{D}_1$. On the other hand $g(p) \in \mathcal{D}_{m+1}$. So, the

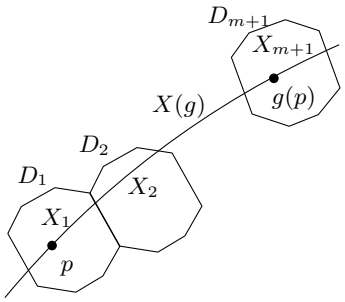

Figure 15: The regions $\mathcal{D}_1, \mathcal{D}_2, \ldots, \mathcal{D}_{m+1}$ cover the segment $[p, g(p)]$.

Dirichlet regions $g\mathcal{D}_1$ and $\mathcal{D}_{m+1}$ are adjacent or coincide. Without loss of generality we assume that $g\mathcal{D}_1 = \mathcal{D}_{m+1}$, since we can always choose a covering of $[p, g(p)]$ satisfying this property. Now let us consider the segments $X_i = X_g \cap \mathcal{D}_i, i \in \{1, \ldots, m+1\}$. We can cover the whole axis X_g by images of these segments under $\mathcal{G}$: any point on the axis X_g is in some segment $g^j[p, g(p)], j \in \mathbb{Z}$, which is covered by the images $\{g^j X_i \mid i \in \{1, \ldots, m+1\}\}$. Moreover, we can cover the axis of any conjugate element $hg\overline{h}$ by images of the segments $X_i, i \in \{1, \ldots, m+1\}$ under $\mathcal{G}$, since the axis $X_{hg\overline{h}}$ is the image of X_g under h. For each X_i, there exists a unique $h_i \in \mathcal{G}$ that sends X_i to $\mathcal{D}_O(\mathcal{G})$, and the set $\{h_i(X_i)\}$ is finite. If the axis of an element of $[g]$ intersects $\mathcal{D}_O(\mathcal{G})$, the intersection segment is the image of some X_i under an element of $\mathcal{G}$ which can only be h_i. Thus the number of axes of the elements of $[g]$ that intersect $\mathcal{D}_O(\mathcal{G})$ is finite. Note that since $\mathcal{D}_{m+1} = g\mathcal{D}_1$ and $X_g = g(X_g)$, we have that $X_{m+1} = gX_1$, i.e., $h_{m+1} = \overline{g}$. □

We have chosen a representative $g \in [g]_O$. We set $X_1 = X_g \cap \mathcal{D}_O(\mathcal{G})$. When X_g leaves $\mathcal{D}_O(\mathcal{G})$, it enters an adjacent region, i.e. there is some $h \in \{a, b, c, d, \overline{a}, \overline{b}, \overline{c}, \overline{d}\}$, for which $X_g \cap h(\mathcal{D}_O(\mathcal{G})) \neq \emptyset$. We set $X_2 = X_g \cap h(\mathcal{D}_O(\mathcal{G}))$. Obviously, $h_2 = \overline{h}$ sends X_2 to $\mathcal{D}_O(\mathcal{G})$. We take $g_2 = h_2 g \overline{h}_2$, then $X_{g_2} \cap \mathcal{D}_O(\mathcal{G}) = h_2(X_2)$.

We pursue the same process inductively. At each step we compute g_{i+1} from g_i in a similar way: $h_i(X_i) \subset \mathcal{D}_O(\mathcal{G})$, and the segments $h_i(X_{i-1})$ and $h_i(X_{i+1})$ are in the two regions adjacent to $\mathcal{D}_O(\mathcal{G})$ and traversed by X_{g_i}: $h_i(X_{i-1}) \subset h_i(\mathcal{D}_O(\mathcal{G}))$ (Figure 16). We take $h \in \{a, b, c, d, \overline{a}, \overline{b}, \overline{c}, \overline{d}\}$, such that $X_{g_i} \cap h(\mathcal{D}_O(\mathcal{G})) \neq \emptyset$ and $h \neq h_i$. By construction, $h_i(X_{i+1}) = X_{g_i} \cap h(\mathcal{D}_O(\mathcal{G}))$. The inverse $\overline{h}$ sends

$h_i(X_{i+1})$ to $\mathcal{D}_O(\mathcal{G})$, so, $h_{i+1} = \overline{h}h_i$ sends X_{i+1} to $\mathcal{D}_O(\mathcal{G})$. We take $g_{i+1} = h_{i+1}g\overline{h}_{i+1} = \overline{h}g_ih$. We stop at step j such that $g_{j+1} = g$. Then we have found $[g]_O = \{g_i, 1 \leq i \leq j\}$.

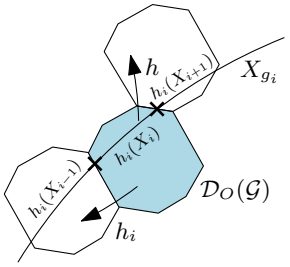

Figure 16: Constructing axes.

We now show the following:

Proposition 31. *The test whether the axes of two elements of $[g]_O$ intersect can be performed exactly using algebraic numbers of degree 2.*

Proof. We first examine the predicate checking whether the axis of a translation g_h of $\mathcal{G}$ intersects $\mathcal{D}_O(\mathcal{G})$, i.e. whether $X_{g_h} \cap \mathcal{D}_O(\mathcal{G}) \neq \emptyset$. This predicate is considered in detail in [3]. We briefly sketch the main steps of the computations here. The axis X_{g_h} of g_h in the Poincaré ball model can be thought of as a Euclidean circle orthogonal to the boundary of the unit disk. The matrix representing g_h in the Poincaré ball model is of the form:

$$\begin{pmatrix} \alpha_1 + i\alpha_2 & \sqrt{\sqrt{2}-1}(\beta_1 + i\beta_2) \\ \sqrt{\sqrt{2}-1}(\beta_1 - i\beta_2) & \alpha_1 - i\alpha_2 \end{pmatrix},$$

where $\alpha_1, \alpha_2, \beta_1\beta_2 \in \mathbb{Q}(\sqrt{2})$. The Euclidean circle corresponding to X_{g_h} is given in Cartesian coordinates by the following equation:

$$x^2 + y^2 - \frac{2\sqrt{\sqrt{2}-1}}{\alpha_2}(\beta_1 y - \beta_2 x) + 1 = 0. \tag{2}$$

The axis X_{g_h} intersects $\mathcal{D}_O(\mathcal{G})$ *iff* the Euclidean circle corresponding to X_{g_h} encloses or contains on the boundary a vertex of $\mathcal{D}_O(\mathcal{G})$. The later boils down to checking whether the following equality holds. $|\alpha_2| \leq (2-\sqrt{2})(|\beta_1| + (\sqrt{2}-1)|\beta_2|)$, where we assume that $|\beta_1| > |\beta_2|$ (this always can be achieved by rotation of the circle over $\frac{\pi}{4}$ around the origin).

Now let us come back to the test whether the axes of two $g_j, g_k \in [g]_O$ intersect. The axes X_{g_j} and X_{g_k} intersect if and only if the corresponding Euclidean circles C_j and C_k intersect. The equation of the Euclidean circle (Equation (2)) can be rewritten as follows:

$$\left(x + \frac{\sqrt{\sqrt{2}-1}}{\alpha_2}\beta_2\right)^2 + \left(y - \frac{\sqrt{\sqrt{2}-1}}{\alpha_2}\beta_1\right)^2 = (\sqrt{2}-1)\frac{(\beta_2^2 + \beta_1^2)}{\alpha_2^2} - 1. \tag{3}$$

Let the equation of C_j be defined by $\alpha_{j_2}, \beta_{j_1}, \beta_{j_2} \in \mathbb{Q}(\sqrt{2})$ substituting respectively $\alpha_2, \beta_1, \beta_2$ in Equation (3). Similarly, let the equation of C_k be defined by $\alpha_{k_2}, \beta_{k_1}, \beta_{k_2} \in \mathbb{Q}(\sqrt{2})$. The squared radius r_j^2 of C_j is

$$r_j^2 = (\sqrt{2}-1)\frac{(\beta_{j_2}^2 + \beta_{j_1}^2)}{\alpha_{j_2}^2} - 1.$$

The squared radius r_k^2 of C_k is similar. The coordinates of the center of each circle are explicitly presented in Equation (3). The squared distance between the centers of C_j, C_k, which we denote by d_{jk}^2, can be deduced using the coordinates of the centers of C_j, C_k and is equal

$$d_{jk}^2 = (\sqrt{2}-1)\left(\left(\frac{\beta_{j_2}}{\alpha_{j_2}} - \frac{\beta_{k_2}}{\alpha_{k_2}}\right)^2 + \left(\frac{\beta_{k_1}}{\alpha_{k_2}} - \frac{\beta_{j_1}}{\alpha_{j_2}}\right)^2\right).$$

Table 2: $L|_{13.24}$

#	length	mult.
0	3.0571	24
1	4.8969	24
2	5.8280	48
3	6.1143	24
4	7.2632	48
5	7.5957	8
6	7.8807	96
7	8.7028	48
8	8.8715	96
9	9.0271	12
10	9.1714	24
11	9.7511	48
12	9.7938	24
13	10.2	96
14	10.2815	96

#	length	mult.
15	10.7004	96
16	10.8758	48
17	10.9343	96
18	11.5566	48
19	11.6561	48
20	11.7509	144
21	11.928	96
22	12.1543	96
23	12.2286	24
24	12.2708	48
25	12.5888	48
26	12.7306	48
27	12.7771	192
28	13.0846	96
29	13.1428	48
30	13.2147	96

Note that both r_j^2, r_k^2 and d_{jk}^2 are in $\mathbb{Q}(\sqrt{2})$.

The circles C_j, C_k intersect if and only if $d_{jk}^2 \leq (r_j + r_k)^2$. The later is equivalent to $d_{jk}^2 - r_j^2 - r_k^2 \leq 2r_j r_k$, and by squaring we come to the condition:

$$(d_{jk}^2 - r_j^2 - r_k^2)^2 \leq 4r_j^2 r_k^2.$$

The predicate whether X_{g_j}, X_{g_k} intersect boils down to the evaluation of this condition that uses only algebraic numbers of degree 2, and thus can be evaluated exactly. □

The method was implemented in C++.[3] Actually, it computes more generally the number of self-intersections of closed geodesics that are present in the length spectrum $L(\mathcal{G})$. Table 2 shows $L|_{13.24}$, which we are more specifically interested in here. Our code also computes representatives of the corresponding conjugacy classes in $\mathcal{L}_0$.[4]

$\mathcal{L}_\cup$ — 2-cycles as unions of two 1-cycles.
The following proposition states that considering either $[g]$ or $[tgt^{-1}]$, for $g \in \mathcal{G}, t \in T(2,3,8)$, has the same geometric meaning.

Proposition 32. *Let ς be a 2-cycle in $\pi(DT_{\mathbb{H}}(\mathcal{GP}))$ and $[g], g \in \mathcal{G}$, be the corresponding conjugacy class in $\mathcal{G}$. For $t \in T(2,3,8)$, there exists a point set $\mathcal{S} \subset \mathbb{H}^2$, such that $\pi(DT_{\mathbb{H}}(\mathcal{GS}))$ has a 2-cycle corresponding to the conjugacy class $[tgt^{-1}]$.*

Proof. Let us take $S = t\mathcal{P}$. Since $\mathcal{G}$ is normal in $T(2,3,8)$, then $DT_{\mathbb{H}}(\mathcal{G}S) = DT_{\mathbb{H}}(\mathcal{G}t\mathcal{P}) = DT_{\mathbb{H}}(t\mathcal{GP}) = tDT_{\mathbb{H}}(\mathcal{GP})$ because t is an isometry.

Let $\widetilde{\varsigma}$ be a lift of ς in $DT_{\mathbb{H}}(\mathcal{GP})$, with endpoints $p \in \mathcal{P}$ and $g(p)$. The image $t(\widetilde{\varsigma})$ is in $DT_{\mathbb{H}}(\mathcal{GS})$ and its endpoints $t(p)$ and $tg(p)$ are in the same $\mathcal{G}$-orbit, thus the projection $\pi(t(\widetilde{\varsigma}))$ is a 2-cycle in $\pi(DT_{\mathbb{H}}(\mathcal{GS}))$. It corresponds to the conjugacy class $[tgt^{-1}]$. □

Let e_1, e_2 be two edges of $DT_{\mathbb{H}}(\mathcal{GP})$ sharing an endpoint, and such that $\pi(e_1) \cup \pi(e_2)$ is a 2-cycle consisting of two 1-cycles in $\pi(DT_{\mathbb{H}}(\mathcal{GP}))$. Let p and $g_i(p)$ be the endpoints of e_i, for $i = 1, 2$, where $p \in \mathbb{H}^2$. For $g_1, g_2 \in \mathcal{G}$, the translation $g_1\overline{g}_2$ sends the endpoint $g_2(p)$ of the union $e_1 \cup e_2$ to its other endpoint $g_1(p)$. We are going to figure out for which elements g_1, g_2 this is possible. Note that both g_1, g_2 are in $C(p)$, and Proposition 10 implies that both g_1, g_2 are in $C(O')$ for some $O' \in T(2,3,8)O$.

[3] http://www-sop.inria.fr/members/Mikhail.Bogdanov/files/main.cpp.
[4] http://www-sop.inria.fr/members/Mikhail.Bogdanov/files/words0

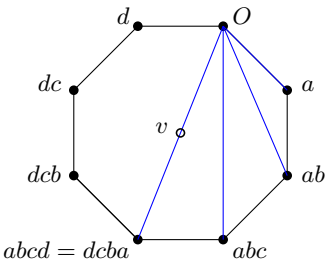

Figure 17: Edges from $p = O$.

Assume for the purpose of illustration that $p = O$. First consider edge $e_1 = [O, g_1]$. Since g_1 is in $C(O)$, e_1 connects two vertices of some octagon $\rho^{k_1}\mathcal{D}_v(\mathcal{G})$, where $0 \leq k_1 < 8$. We can assume that $k_1 = 0$, otherwise by Proposition 32 we can consider $\rho^{-k_1} g_1 \rho^{k_1}$ instead of g_1. Then $g_1 \in F\backslash\{\mathbb{1}\}$. Then we note that $d, dc, dcb, dcba$ are the respective conjugates of $a, ab, abc, abcd$ by the reflection in the line passing through O and $abcd$ (Figure 17). Thus by Proposition 32 it is sufficient to consider only $g_1 \in \{a, ab, abc, abcd\}$.

Now let us consider edge $e_2 = [O, g_2]$. The endpoints of e_2 are vertices of $\rho^{k_2} D_v(\mathcal{G})$ for some $0 \leq k_2 < 8$ and h be the translation of $\mathcal{G}$ that sends e_2 in the Dirichlet region $\mathcal{D}_v(\mathcal{G})$. By definition of $DT_{\mathbb{H}}(\mathcal{GP})$ the image $h(e_2) = e_2'$ is an edge of $DT_{\mathbb{H}}(\mathcal{GP})$. The edges e_2' and e_1 do not intersect.

Proposition 33. *Let g_1, g_2 be in $C(O)$. Let h be the translation in $\mathcal{G}$ such that the geodesic segments $[O, g_1]$ and $[h, hg_2]$ intersect transversally. Then for any $p \in \mathbb{H}^2$ the projections of the geodesic segments $[p, g_1(p)]$ and $[h(p), hg_2(p)]$ on $\mathcal{M}$ intersect transversally.*

Proof. Let f denote the translation $g_1\overline{g}_2$. Let γ' denote the union of segments $[O, g_2]$ and $[O, g_1]$. Note that f maps the endpoint g_2 to the endpoint g_1. Let λ' denote the polygonal chain obtained as the union $\cup_{k\in\mathbb{Z}} f^k(\gamma')$. The vertices of λ' lie on two curves that have constant distance to the axis X_f of the translation f.

Similarly let γ'' denote the union of segments $[h, hg_1]$ and $[h, hg_2]$. The endpoint hg_2 is mapped to the endpoint hg_1 by $hf\overline{h}$. Let λ'' denote the polygonal chain obtained as the union $\cup_{k\in\mathbb{Z}}(hf\overline{h})^k(\gamma'')$. The chain λ'' is the image of λ' under h. The vertices of λ'' lie on two curves that have constant distance to the axis $X_{hf\overline{h}}$ of $hf\overline{h}$. These curves are images of the curves corresponding to λ' under h.

The chains λ' and λ'' intersect transversally at $[O, g_1] \cap [h, hg_2]$. This point of $\lambda' \cap \lambda''$ is unique, otherwise their corresponding curves intersect more than in one point. Thus $X_f \cap X_{hf\overline{h}} \neq \emptyset$. In a similar way, we can construct polygonal chains for $[p, g_1(p)]$ and $[h(p), hg_2(p)]$. These polygonal chains must intersect since they have common points at infinity with X_f and $X_{hf\overline{h}}$ respectively. Their intersection point corresponds to the intersection point of the projections of $[p, g_1(p)]$ and $[h(p), hg_2(p)]$ on $\mathcal{M}$. □

Proposition 33 allows us to enumerate all possible e_2' with endpoints at vertices of $\mathcal{D}_v(\mathcal{G})$ so that e_1 and

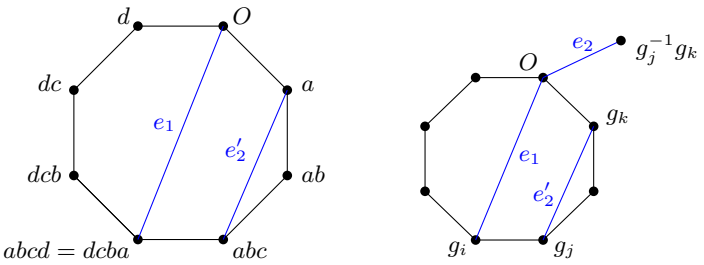

Figure 18: Enumerating edges.

e_2' do not intersect (Figure 18(left)). Let us consider $e_1 = [O, g_i]$ and $e_2' = [g_j, g_k]$, where $g_i, g_j, g_k \in F$. Without loss of generality assume that e_2' is the image of e_2 under the (unique) translation of $\mathcal{G}$ that sends O to g_j. Then clearly the endpoints of e_2 are O and $\overline{g}_j g_k$ (Figure 18(right)). Then $e_1 \cup e_2$ projects to a 2-cycle since g_i and $\overline{g}_j g_k$ are on the same $\mathcal{G}$-orbit.

The function `generate_words_union_1_cycles` implements that enumeration of elements $g_i\overline{g}_k g_j$ for which e_1 and e'_2 do not intersect.[5] It allows to compute the list $\mathcal{L}_\cup$ of representatives of conjugacy classes corresponding to unions of 1-cycles.[6]

Subgroups not containing elements of $\mathcal{L} = \mathcal{L}_0 \cup \mathcal{L}_\cup$.
The idea of the method is simplistic: we consider one by one the groups that are available at [16], and check using GAP whether they are subgroups of $\mathcal{G}$ and whether they contain an element of $\mathcal{L}$.

More precisely, the subgroups listed at [16] are quotient groups $T(2,m,n)/G$ where G is a normal subgroup of $T(2,m,n)$ acting on $\mathbb{H}^2$ witout fixed points. They are ordered by genus of the corresponding surface $\mathbb{H}^2/G$, up to genus 301 [17]. $\mathcal{G}$ is one of them. Considering normal subgroups in $T(2,m,n)$ allows us to expect to get covering spaces of $\mathcal{M}$ that preserve symmetries of the octagon. The method was implemented using GAP.[7] The program actually does not find any suitable subgroup of $\mathcal{G}$.

However, while carefully examining its output, we notice that there is a unique subgroup $\mathcal{G}_{128}$ of $\mathcal{G}$ of index 128 that is normal in $T(2,3,8)$, and it does not contain any element of $\mathcal{L}$, except $(abcd)^2$.

The group $\mathcal{G}_{128}$ is defined in the following way. We use the finitely presented form of $T(2,3,8)$ [33, 27]:

$$T(2,3,8) =< R,S,T \mid R^3, S^8, T^2, (R\cdot S)^2, (R\cdot T)^2, (S\cdot T)^2 > .$$

With the same notation, V denotes the following set of elements [16]

$$\begin{aligned} V \quad = \quad & \{R^3, S^8, T^2, (R\cdot S)^2, (R\cdot T)^2, (S\cdot T)^2, \\ & S\cdot R\cdot S^-3\cdot R^-1\cdot S\cdot R^-1\cdot S^-4\cdot R\cdot S^-1\cdot R\cdot S^4\cdot R\cdot S^-1\cdot R\cdot S^-3\cdot R\cdot S^2, \\ & S^-1\cdot R\cdot S^-2\cdot R^-1\cdot S^2\cdot R\cdot S^-2\cdot R\cdot S^-2\cdot R^-1\cdot S\cdot R^-1\cdot S^-2\cdot R\cdot S^2\cdot R^-1\cdot S^2\cdot R^-1\cdot S^-2\}. \end{aligned}$$

Let now N be the group

$$N =< R,S,T \mid V > .$$

N is finite [17]. Then $\mathcal{G}_{128} = T(2,3,8)/N$.

Provided that this result, obtained by running software is considered as "proved", we show the following:

Proposition 34. *For any set of points $\mathcal{P}$, the graph of edges of the projection of $DT_{\mathbb{H}}(\mathcal{GP})$ to $\mathbb{H}^2/\mathcal{G}_{128}$ has no 2-cycle.*

Proof. A potential 2-cycle corresponding to $(abcd)^2$ would be formed by the projections of two edges: the edge incident to p and $abcd(p)$ and the edge incident to $abcd(p)$ and $(abcd)^2(p)$, for some $p \in \mathcal{P}$.

If p is the origin O, each of these edges is the diameter of a largest ball that contains no point of $\mathcal{G}O$ in its interior. The same reasoning as in the Euclidean case (see Proposition 18) shows that, if the point set $\mathcal{P}$ contains the origin O and at least one more point, then the projection of $DT_{\mathbb{H}}(\mathcal{GP})$ to $\mathbb{H}^2/\mathcal{G}_{128}$ has no 2-cycle. Actually, even if $\mathcal{P} = \{O\}$, it is always possible to triangulate the fundamental domain $\mathcal{D}_v(\mathcal{G})$ in such a way that no pair of opposite vertices form an edge; the triangulation of $\mathbb{H}^2/\mathcal{G}_{128}$ induced by this triangulation has no 2-cycle.

If $p \neq O$, Observation 9 shows that the edge with vertices p and $abcd(p)$ cannot be an edge of $DT_{\mathbb{H}}(\mathcal{GP})$. So, if $\mathcal{P}$ does not contain O, then the projection of $DT_{\mathbb{H}}(\mathcal{GP})$ to $\mathbb{H}^2/\mathcal{G}_{128}$ again does not contain a 2-cycle. □

6 Triangulating the Bolza surface in practice

As done for Euclidean manifolds [12, 11, 13], the incremental algorithm for computing a Delaunay triangulation can be used in a covering space of $\mathcal{M}$ in which the graph of its edges is a simplicial comlex, i.e., it has no 2-cycles. It would obviously be of low practical interest to compute in $\mathbb{H}^2/\mathcal{G}_{128}$, since we would have to consider 128 images of $\mathcal{P}$. Instead, we can initialize the triangulation with a well chosen set $\mathcal{Q}$ of 14 points for which $sys(\mathcal{M}) > 2\delta_{\mathcal{Q}}$. By Proposition 4(2), this ensures that the triangulation of $\mathcal{Q}\cup\mathcal{P}$ on $\mathcal{M}$ will have no 2-cycle, for any $\mathcal{P}$.

[5] http://www-sop.inria.fr/members/Mikhail.Bogdanov/files/main.cpp
[6] http://www-sop.inria.fr/members/Mikhail.Bogdanov/files/union_loops
[7] http://www-sop.inria.fr/members/Mikhail.Bogdanov/files/subgroups48.gwp

The rest of this section presents the set $\mathcal{Q}$.

The group $\mathcal{G}$ is a normal subgroup without fixed point of index 48 in the triangle group $T(2,4,8)$. The partition of the octagon $\mathcal{D}_O(\mathcal{G})$ into 48 triangles with angles $\pi/2, \pi/4, \pi/8$ that are fundamental domains for $T(2,4,8)$ is shown in Figure 19(left). Let Δ be a triangle of the partition that is incident to the origin. The set of vertices of Δ is denoted by $\mathcal{Q}_T$. We take the set $\mathcal{Q} = T(2,4,8)\mathcal{Q}_T \cap \mathcal{D}_O(\mathcal{G})$. Note that $T(2,4,8)\mathcal{Q}_T = \mathcal{G}\mathcal{Q}$. Consider the image of Δ by the reflection along its side opposite to the

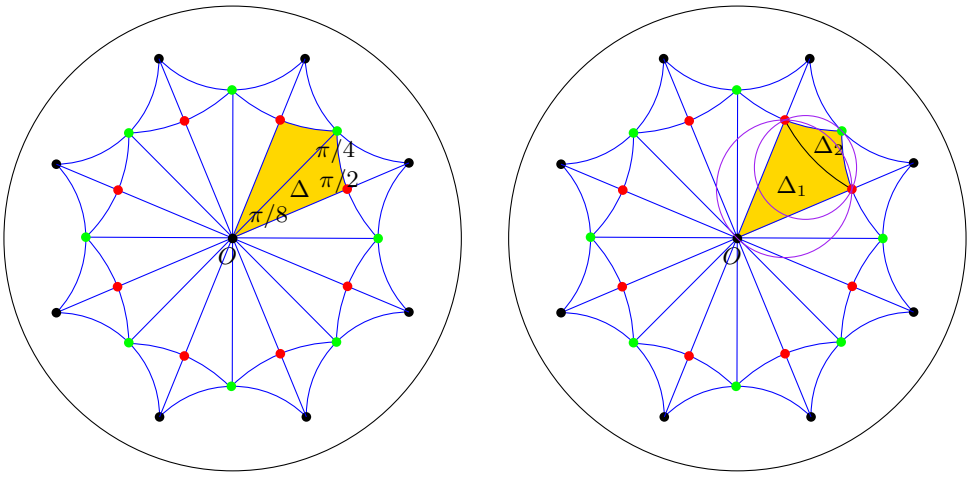

Figure 19: (left) Partition of $\mathcal{D}_O(\mathcal{G})$ into fundamental domains for $T(2,3,8)$. (right) Triangles Δ_1, Δ_2 obtained by edge-flipping.

vertex with angle $\pi/2$. Flipping the edge shared by these two triangles gives us two new triangles Δ_1 and Δ_2 (See Figure 19(right)). The circumscribing balls of Δ_1 and Δ_2 contain no point of $T(2,4,8)\mathcal{Q}_T$ in their interiors. Note that $\Delta_1 \cup \Delta_2$ is a fundamental domain for the subgroup $T^+(2,4,8)$ of orientation-preserving isometries of $T(2,4,8)$, and therefore the hyperbolic plane $\mathbb{H}^2$ is covered by the images of $\Delta_1 \cup \Delta_2$ under $T^+(2,4,8)$. This partition of $\mathbb{H}^2$ gives us the Delaunay triangulation of $\mathbb{H}^2$ defined by the set $T(2,4,8)\mathcal{Q}_T$. In fact, we get the triangulation $\mathrm{DT}_{\mathbb{H}}(\mathcal{G}\mathcal{Q})$, since $T(2,4,8)S_T = \mathcal{G}S$.

Let $\delta_{\mathcal{Q}}$ denote the largest empty ball diameter with respect for the set $\mathcal{G}\mathcal{Q}$, and d_1, d_2 denote the diameters of the balls circumscribing Δ_1, Δ_2 respectively. There is a triangle in $\mathrm{DT}_{\mathbb{H}}(\mathcal{G}\mathcal{Q})$ whose circumscribing ball is of diameter $\delta_{\mathcal{Q}}$. Since any triangle in $\mathrm{DT}_{\mathbb{H}}(\mathcal{G}\mathcal{Q})$ is the image of Δ_1 or Δ_2 under some isometry of $T^+(2,4,8)$, either d_1 or d_2 is equal to $\delta_{\mathcal{Q}}$. Both diameters d_1 and d_2 are less than $\frac{1}{2}sys(\mathcal{M})$, which actually is the radius of the inscribed circle in $\mathcal{D}_O(\mathcal{G})$. So the largest empty ball diameter $\delta_{\mathcal{Q}}$ is less than $\frac{1}{2}sys(\mathcal{M})$. Inserting new points in the triangulation cannot increase the size of empty balls, i.e., $\delta_{\mathcal{P}\cup\mathcal{Q}} \leq \delta_{\mathcal{Q}}$ for any set $\mathcal{P}$, so by Proposition 4, $\pi(\mathrm{DT}_{\mathbb{H}}(\mathcal{G}\mathcal{P} \cup \mathcal{Q}))$ has no 2-cycle.

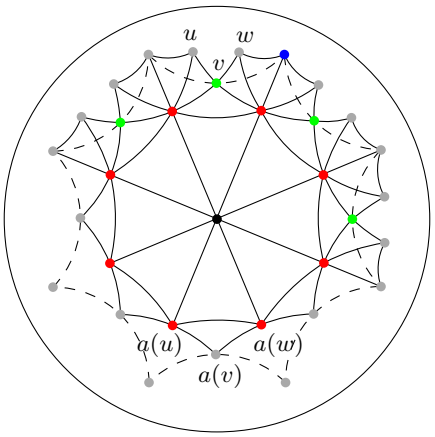

Figure 20: The set $\mathcal{Q}$.

Figure 20 shows unique representatives in $\mathbb{H}^2$ of the triangles of $\pi(\mathrm{DT}_{\mathbb{H}}(\mathcal{GQ}))$. The point set $\mathcal{Q}$ contains 9 points in the interior of $\mathcal{D}_O$ (origin and red points), 4 points on the boundary of $\mathcal{D}_O$ (green points) and 1 point at its vertex (blue point). In total $\mathcal{Q}$ consists of 14 points.

Acknowledgements

The authors warmly thank Gert Vegter for early discussions on the construction of covering spaces of the Bolza surface.

References

[1] Mark A. Armstrong. *Basic Topology*. Springer-Verlag, 1982.

[2] M. Artin. *Algebra*. Prentice-Hall, New Delhi, India, 2002.

[3] R. Aurich, E. B. Bogomolny, and F. Steiner. Periodic orbits on the regular hyperbolic octagon. *Physica D: Nonlinear Phenomena*, 48(1):91–101, 1991.

[4] Agnès Bachelot-Motet. Wave computation on the hyperbolic double doughnut. *Journal of Computational Mathematics*, 28:1–17, 2010.
http://www.academia.edu/4674754/Wave_Computation_on_the_Hyperbolic_Double_Doughnut.

[5] M. Berger. *Geometry (vols. 1-2)*. Springer-Verlag, 1987.

[6] Mikhail Bogdanov, Olivier Devillers, and Monique Teillaud. Hyperbolic Delaunay complexes and Voronoi diagrams made practical. In *Proc. of the 29th Annual Symposium on Computational Geometry*, pages 67–76, 2013.
http://hal.inria.fr/hal-00833760.

[7] Mikhail Bogdanov, Monique Teillaud, and Gert Vegter. Covering spaces and Delaunay triangulations of the 2d flat torus. In *Abstracts 28th European Workshop on Computational Geometry*, pages 9–12, 2012.
http://www.diei.unipg.it/eurocg2012/booklet.pdf.

[8] P. Buser. *Geometry and Spectra of Compact Riemann Surfaces*. Progress in Mathematics Series. Birkhäuser, 1992.

[9] P. Buser and P. Sarnak. On the period matrix of a Riemann surface of large genus (with an Appendix by J.H. Conway and N.J.A. Sloane). *Inventiones mathematicae*, 117:27–56, 1994.
http://dx.doi.org/10.1007/BF01232233.

[10] James W. Cannon, William J. Floyd, Richard Kenyon, and Walter R. Parry. Hyperbolic geometry. *Flavors of geometry*, 31:59–115, 1997.
http://www.math.uwo.ca/~shafikov/teaching/winter2010/4156/hyperbolic.pdf.

[11] Manuel Caroli. *Triangulating Point Sets in Orbit Spaces*. Thèse de doctorat en sciences, Université de Nice-Sophia Antipolis, France, 2010.
http://tel.archives-ouvertes.fr/tel-00552215/.

[12] Manuel Caroli and Monique Teillaud. Computing 3D periodic triangulations. In *Proceedings 17th European Symposium on Algorithms*, volume 5757 of *Lecture Notes in Computer Science*, pages 37–48, 2009.
http://hal.inria.fr/inria-00356871/.

[13] Manuel Caroli and Monique Teillaud. Delaunay triangulations of point sets in closed Euclidean d-manifolds. In *Proceedings 27th Annual Symposium on Computational Geometry*, pages 274–282, 2011.

[14] Manuel Caroli and Monique Teillaud. 3D periodic triangulations. In *CGAL User and Reference Manual*. CGAL Editorial Board, 4.3 edition, 2013.
http://doc.cgal.org/4.3/Manual/packages.html#PkgPeriodic3Triangulation3Summary.

[15] P. Chossat, G. Faye, and O. Faugeras. Bifurcation of hyperbolic planforms. *Journal of Nonlinear Science*, 21:465–498, 2011.
http://link.springer.com/article/10.1007%2Fs00332-010-9089-3.

[16] Marston Conder. Regular orientable maps of genus 2 to 301, 2012.
http://http://www.math.auckland.ac.nz/~conder/OrientableRegularMaps301.txt.

[17] Marston Conder and Peter Dobcsányi. Determination of all regular maps of small genus. *Journal of Combinatorial Theory, Series B*, 81(2):224–242, 2001.

[18] The GAP Group. *GAP – Groups, Algorithms, and Programming, Version 4.6.5*, 2013.
http://www.gap-system.org.

[19] Mikhael Gromov. Filling Riemannian manifolds. *J. Differ. Geom.*, 18:1–147, 1983.

[20] Mikhael Gromov. Systoles and intersystolic inequalities. In *Actes de la Table Ronde de Géométrie Différentielle (Luminy, 1992)*, volume 1 of *Sémin. Congr.*, pages 291–362. Soc. Math. France, Paris, 1996.

[21] M.K. Hurdal and K. Stephenson. Cortical cartography using the discrete conformal approach of circle packings. *Neuroimage*, 23:119–128, 2004.

[22] S. Katok. *Fuchsian Groups*. Chicago Lectures in Mathematics. University of Chicago Press, 1992.

[23] Nico Kruithof. 2D periodic triangulations. In *CGAL User and Reference Manual*. CGAL Editorial Board, 4.3 edition, 2013.
http://doc.cgal.org/4.3/Manual/packages.html#PkgPeriodic2Triangulation2Summary.

[24] Anatoliı I Malcev. On the faithful representation of infinite groups by matrices. *Mat. Sb*, 8(50):405–422, 1940.

[25] Marjatta Naatanen. On the stability of identification patterns for Dirichlet regions. *Annales Academiæ Scientiarum Fennicæ, Series A. I. Mathematica*, 10:411–417, 1985.

[26] Henri Poincaré. Analysis situs. *J. Ecole Polytechn.*, 2(1):1–121, 1895.

[27] J. Ratcliffe. *Foundations of Hyperbolic Manifolds*. Number vol. 10 in Graduate Texts in Mathematics. Springer, 2006.

[28] Guodong Ron, Miao Jin, and Xiaohu Guo. Hyperbolic centroidal Voronoi tessellation. In *Proc. ACM Symposium on Solid and Physical Modeling*, pages 117–126, Haifa, Israel, 2010.

[29] François Sausset, Gilles Tarjus, and Pascal Viot. Tuning the fragility of a glassforming liquid by curving space. *Physical Review Letters*, 101:155701(1)–155701(4), 2008.
http://dx.doi.org/10.1103/PhysRevLett.101.155701.

[30] Peter Scott. Subgroups of surface groups are almost geometric. *Journal of the London Mathematical Society*, 2(17):555–565, 1978.

[31] I.R. Shafarevich. *Basic notions of algebra*. Encyclopaedia of mathematical sciences. Springer, 2005.

[32] C.C. Sims. *Computation with Finitely Presented Groups*. Encyclopedia of Mathematics and its Applications. Cambridge University Press, 1994.

[33] J. Stillwell. *Geometry of surfaces*. Universitext (1979). Springer-Verlag, 1992.

[34] W. P. Thurston. Three dimensional manifolds, Kleinian groups, and hyperbolic geometry. *Bull. Amer. Math. Soc.*, 6(3):357–381, 1982.
http://www.ams.org/mathscinet-getitem?mr=648524.

[35] William P. Thurston. *The Geometry and Topology of Three-Manifolds*. 2002.
http://www.msri.org/publications/books/gt3m/.

[36] P M. H. Wilson. *Curved Spaces*. Cambridge University Press, Cambridge, 2008.

Contents

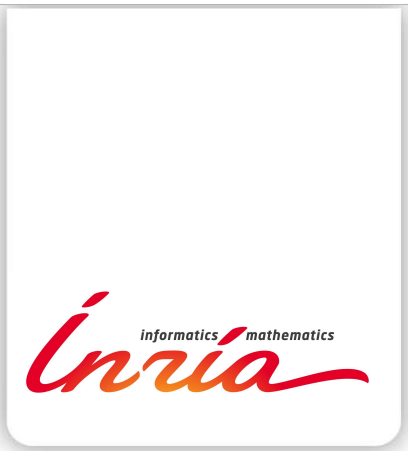

RESEARCH CENTRE
SOPHIA ANTIPOLIS – MÉDITERRANÉE

2004 route des Lucioles - BP 93
06902 Sophia Antipolis Cedex

Publisher
Inria
Domaine de Voluceau - Rocquencourt
BP 105 - 78153 Le Chesnay Cedex
inria.fr

ISSN 0249-6399